Molecular Pharmacology Fast Forward. Published on April 1, 2021 as DOI: 10.1124/molpharm.120.000191
This article has not been copyedited and formatted. The final version may differ from this version.

Inhibition of hUNG Sensitizes a Large Fraction of Colorectal Cancer Cells to 5-fluorodeoxyuridine (FdU) and Raltitrexed (RTX) but not Fluorouracil (FU)

Eric S. Christenson, Anthony Gizzi, Junru Cui, Matthew Egleston, Kyle J. Seamon, Michael DePasquale, Benjamin Orris, Ben H. Park, and James T. Stivers*

Department of Pharmacology and Molecular Sciences, Johns Hopkins University School of Medicine 725 North Wolfe Street Baltimore, MD 21205 (ESC, AG, JC, ME, KS, BO, JTS)

Lieber Institute for Brain Development, 855 North Wolfe Street Baltimore, MD 21205 (MD)

Vanderbilt University Medical Center/Vanderbilt-Ingram Cancer Center, 2220 Pierce Ave. PRB Room 777 Nashville, TN 37232 (BHP)

Molecular Pharmacology Fast Forward. Published on April 1, 2021 as DOI: 10.1124/molpharm.120.000191
This article has not been copyedited and formatted. The final version may differ from this version.

Running Title Page

Running Title: Inhibition of hUNG potentiates FdU killing in cancer cells

Contact information for corresponding author: James T. Stivers, Department of Pharmacology and Molecular Sciences, Johns Hopkins University School of Medicine 725 North Wolfe Street Baltimore, MD 21205, *jstivers@jhmi.edu,* 410-292-6844

Number of text pages: 38

Number of tables: 0

Figures: 8

References: 37

Abstract: 245 words

Introduction: 720 words

Discussion: 1528 words

Non-standard abbreviations:

A3B, Apobec DNA cytidine deaminase B
APE1, apurinc/apyrimidinic endonuclease 1
BRCA1, breast cancer protein 1
BRCA2, breast cancer protein 2
DPD, dihydrophyrimidine dehydrogenase
dU, deoxyuridine
DUT, deoxyuridine triphosphate nucleotidyl hydrolase
FdU, fluorodeoxyuridine
FU, fluorouracil
FdUMP, fluorodeoxyuridine 5' monophosphate
FUDP, 5-fluorouridine 5' diphosphate
FUTP, 5-fluorouridine 5' triphosphate
FdUDP, 5-fluorodeoxyuridine 5' diphosphate
FdUTP, 5-fluorodeoxyuridine 5' triphosphate
hUNG, human uracil DNA glycosylase
Lig III ,DNA ligase III

Molecular Pharmacology Fast Forward. Published on April 1, 2021 as DOI: 10.1124/molpharm.120.000191
This article has not been copyedited and formatted. The final version may differ from this version.

MLH1, mut L human homologue 1

MSH2, mut S human homologue 2

MSH6, mut S human homologue 6

NMPK, nucleoside monophosphate kinase

NDPK, nucleoside diphosphate kinase

OPRT, orotate phosphoribosyltransferase

Pol β, DNA polymerase β

Pol ε, DNA polymerase epsilon

Pol δ, DNA polymerase delta

R, hUNG responsive

NR, hUNG non-responsive

RNR, ribonucleotide reductase

RNAP III, RNA polymerase III

RTX, raltitrexed

SAMHD1, sterile alpha motif histidine-aspartate domain containing deoxynucleoside triphosphate triphosphohydrolase 1

SMUG1, single strand mismatch DNA glycosylase

TK, thymidine kinase

TS, thymidylate synthase

TDG, thymidine DNA glycosylase

TP, thymidine phosphorylase

UGI, uracil DNA glycosylase inhibitor protein

Molecular Pharmacology Fast Forward. Published on April 1, 2021 as DOI: 10.1124/molpharm.120.000191
This article has not been copyedited and formatted. The final version may differ from this version.

Abstract

Previous shRNA knockdown studies have established that depletion of human uracil DNA glycosylase (hUNG) sensitizes some cell lines to 5-fluorodeoxyuridine (FdU). Here we selectively inhibit the catalytic activity of hUNG by lentiviral transduction of UNG inhibitor protein (UGI) into a large panel of cancer cell lines under control of a doxycycline-inducible promoter. This induced inhibition strategy better assesses the therapeutic potential of small molecule targeting of hUNG. In total, six of eleven colorectal lines showed 6 to 70-fold increases in FdU potency upon hUNG inhibition ("responsive"). This hUNG dependent response was not observed with fluorouracil (FU), indicating that FU does not operate through the same DNA repair mechanism as FdU in vitro. Potency of the thymidylate synthase inhibitor raltitrexed (RTX), which elevates dUTP levels, was only incrementally enhanced upon hUNG inhibition (<40%), suggesting that responsiveness is associated with incorporation and persistence of FdU in DNA rather than dU. The importance of FU/A and FU/G lesions in toxicity of FdU is supported by the observation that dT supplementation completely rescued the toxic effects of U/A lesions resulting from RTX, but dT only increased the IC_{50} for FdU, which forms both FU/A and FU/G mismatches. Contrary to previous reports, cellular responsiveness to hUNG inhibition did not correlate with p53 status or thymine DNA glycosylase expression. A model is suggested where the persistence of FU/A and FU/G base pairs in the absence of hUNG activity elicits an apoptotic DNA damage response in both responsive and non-responsive colorectal lines.

Molecular Pharmacology Fast Forward. Published on April 1, 2021 as DOI: 10.1124/molpharm.120.000191
This article has not been copyedited and formatted. The final version may differ from this version.

Significance Statement. The pyrimidine base 5-fluorouracil is a mainstay chemotherapeutic for treatment of advanced colorectal cancer. Here we show that its deoxynucleoside form, 5-fluorodeoxyuridine (FdU), operates by a distinct DNA incorporation mechanism that is strongly potentiated by inhibition of the DNA repair enzyme uracil DNA glycosylase (hUNG). The UNG-dependent mechanism was present in over 50% of colorectal cell lines tested, suggesting that a significant fraction of human cancers may be sensitized to FdU in the presence of a small molecule UNG inhibitor.

Molecular Pharmacology Fast Forward. Published on April 1, 2021 as DOI: 10.1124/molpharm.120.000191
This article has not been copyedited and formatted. The final version may differ from this version.

INTRODUCTION

The backbone for treatment of advanced colorectal cancer is the nucleobase analogue fluorouracil (FU) (Benson *et al.*, 2017). The toxicity of FU arises through three major mechanisms (**Fig. 1a**) (i) metabolic conversion into the ribonucleotide triphosphate (FUTP) and incorporation into ribosomal RNA with perturbation of ribosome function (RNA pathway), (ii) conversion into the deoxynucleotide triphosphate, (FdUTP) which is incorporated into DNA and recognized as damage (DNA pathway), and (iii) conversion to the deoxnucleotide monophosphate (FdUMP), which potently inhibits thymidylate synthase (TS)(Longley *et al.*, 2003; Mojardín *et al.*, 2013). This last pathway depletes dTMP pools and the DNA building block dTTP, and also increases the dUTP/dTTP ratio, resulting in a second type of DNA damage due to dUTP incorporation into DNA (**Fig. 1A**). Although FU is the mainstay for treatment of colorectal cancer, this prodrug has pharmacological liabilities because it primarily follows the RNA pathway. The RNA pathway is thought to be the major driver of the dose limiting bone marrow and intestinal epithelial cell toxicities accompanying treatment while the minor DNA pathway is more important in animal models for killing tumors (Houghton *et al.*, 1979; van Groeningen *et al.*, 1989; Pritchard *et al.*, 1997).

Although not widely used in the clinic, the deoxynucleoside form of fluorouracil, 5-fluorodeoxyuridine (FdU), is also an FDA approved drug and showed comparable or greater efficacy in early clinical trials as compared to FU (van Laar *et al.*, 1998). The pharmacologic action of FdU is thought to be dominated by the DNA pathway and its ability to simultaneously deplete dTTP and elevate FdUTP and dUTP pools [although a substantial fraction of FdU may be converted to FU in the liver by the action of thymidine phosphorylase (TP)] (**Fig. 1A**)(Vodenkova *et al.*, 2020). The incorporation of FdU and dU into DNA by replicative DNA polymerases results in damaged bases that are recognized and excised by the DNA repair enzyme uracil DNA glycosylase 2 (hUNG)(Grogan *et al.*, 2011).

Molecular Pharmacology Fast Forward. Published on April 1, 2021 as DOI: 10.1124/molpharm.120.000191
This article has not been copyedited and formatted. The final version may differ from this version.

The distinct mechanism of FdU that leads to DNA damage suggests that different opportunities exist for increasing its efficacy and selectivity for targeting cancer cells as compared to FU. In this regard, the Karnitz group has already established strong synergy between FdU and PARP inhibitors, and the Gerson group has reported that shRNA depletion of hUNG leads to sensitization of p53 mutant cancer cells to FdU (Huehls *et al.*, 2011; Yan *et al.*, 2018). These studies suggest that other interactions in DNA base excision repair or cell checkpoint signaling pathways may yet be identified that increase the therapeutic utility of FdU.

Here we examine the effects of inhibiting hUNG catalytic activity in the context of three drugs: FdU, FU and the selective thymidylate synthase inhibitor raltitrexed (RTX). We explore a large panel of cancer cell lines by using stable lentiviral transduction of the uracil DNA glycosylase inhibitor protein (UGI) derived from bacterial phage PBS2 (Cole *et al.*, 2013). UGI binds with extremely high affinity to the active site of hUNG and potently inhibits its catalytic activity (**Fig. 1B**)(Mol *et al.*, 1995). The mode of action of UGI (MW ~10 kDa) is remarkably similar to well-characterized small molecule inhibitors of hUNG that target its active site and UGI provides a useful tool to evaluate the potential of hUNG for drug targeting (**Fig. 1C**). Previous protein depletion approaches using shRNA or siRNA have an inherent shortcoming because hUNG uses its 90 amino acid non-catalytic N-terminal domain to interact with several DNA replication factors (RPA, PCNA) and the observed effects of depletion could arise from the loss of catalytic function and/or protein-protein interactions that are important for DNA replication (Weiser *et al.*, 2018). The inducible UGI method allows for facile screening of a large panel of cancer cell lines for sensitization to FdU, FU and RTX in the context of hUNG inhibition. We find that over 50% of colorectal cancer cell lines show increased sensitivity to FdU and RTX when hUNG activity is absent (“hUNG responsive”), which is not solely predicted by p53 status. In contrast, the tumor toxicity of FU was completely independent of hUNG activity in all cell lines. Nucleoside rescue, structure-activity correlations, biochemical and mechanism of cell death

Molecular Pharmacology Fast Forward. Published on April 1, 2021 as DOI: 10.1124/molpharm.120.000191
This article has not been copyedited and formatted. The final version may differ from this version.

studies all support the conclusion that the persistence of FdU in DNA, in the absence of hUNG activity, is the primary tumor toxicity mechanism of FdU in responsive and non-responsive cell lines.

MATERIALS AND METHODS

Chemicals. 5-fluorodeoxyuridine (FdU), 5-fluorouracil (FU), raltitrexed (RTX) were obtained from Tocris (Bristol, United Kingdom). 5-bromodeoxyuridine (BrdU) and 5-chlorodeoxyuridine (CldU) were obtained from Sigma-Aldrich (St. Louis, MO).

Proteins and antibodies. UGI and *E. coli* UNG were obtained from New England Biolabs (NEB, Ipswich, MA). Human UNG catalytic domain was expressed in bacteria and purified as previously described (Slupphaug *et al.*, 1995)**.** Purified TDG with a 6x-HisTag was a gift from Dr. Michael Matunis. A recombinant Anti-TDG monoclonal antibody was used for western blotting (Abcam, Cambridge, UK, ab154192) and was validated in CRISPR knockout cell lines (Neri *et al.*, 2015).

DNA oligonucleotides and DNA sequencing. All DNA oligonucleotide primers and substrates were synthesized by Integrated DNA Technologies (IDT, Coralville, IA). Sanger DNA sequencing was performed by the Johns Hopkins University sequencing core. Primer and shRNA guide sequences are listed in **Supplementary Table S1**.

Cell lines. BT474, Cama1, HT29, MCF7, NCI-N87, SKBR3, Snu1, T47D, SW480, SW620, DLD1, HCT15, H460, KM12, LS513, Colo205, HCC2998, LoVo, HepG2 cell lines were from American Type Culture Collection (ATCC, Manassas, VA). HCT116 wild-type and HCT116 TP53 knock out cells were provided by Fred Bunz and AsPC1 cells were provided by James Eshleman. Cells were tested upon receipt and every three months while in culture for mycoplasma using PCR based detection (Applied Biological Materials, Inc. Richmond, BC

Molecular Pharmacology Fast Forward. Published on April 1, 2021 as DOI: 10.1124/molpharm.120.000191
This article has not been copyedited and formatted. The final version may differ from this version.

Cat:G238). Identity of cells was confirmed with Short Tandem Repeat DNA fingerprinting provided by ATCC (Manassas, VA).

Construction of inducible UGI cell lines by lentiviral transduction. The cDNA sequence of the uracil DNA glycosylase inhibitor protein (UGI) derived from bacterial phage PBS2 optimized for human codon usage was synthesized by Integrated DNA Technologies (Coralville, IA). This sequence was inserted into the pENTR4 plasmid from Addgene (Watertown, MA) and transferred into the CW57.1 doxycycline inducible overexpression plasmid (Addgene) using the Gateway recombinase system from Thermofisher (Waltham, MA). Sanger sequencing was performed at the conclusion of each step to confirm the expected product. The CW57.1 UGI plasmid was then transfected into T293-FT cells along with pspax2 and pmd2.g helper vectors (Addgene, Watertown, MA). Over the 96 hours following transfection, the virus-containing supernatant was harvested and concentrated 100-fold. This virus was introduced into a panel of 21 cell lines in addition to an isogenic TP53 knock-out HCT116 cell line (see **Supplemental Table S2**).

RT-qPCR measurements of mRNA expression levels of DNA repair and uracil metabolism associated genes. Colon cancer cell lines of interest were cultured to 80% confluence in a T25 flask. Cells were washed with 2mL of PBS x 1 with the addition of trypsin-EDTA (0.05%) (ThermoFisher, Waltham, MA) until detachment. This cell containing solution was passed through a 35 micron filter (Thermo Fisher, Waltham, MA) to eliminate cell clumps prior to counting via a hemacytometer. 100,000 cells were transferred to a T75 flask. Cells were then allowed to grow for 5 days followed by media removal, washed with PBS x 1 prior to addition of trypsin-EDTA 0.05%. After allowing sufficient time for detachment, this solution was then transferred to a 15 mL conical and spun at 386 g x 10 minutes to pellet cells. Trypsin was removed and pellet washed 3 times with PBS with repeated centrifugation in between wash steps. RNA was extracted from cell pellet using the RNeasy Plus Mini Kit (Qiagen, Hilden,

Molecular Pharmacology Fast Forward. Published on April 1, 2021 as DOI: 10.1124/molpharm.120.000191
This article has not been copyedited and formatted. The final version may differ from this version.

Germany) kit according to the manufacturer's protocol. 3 μg of RNA was used to generated cDNA with the Qiagen OmniScript cDNA preparation kit following the manufacturers protocol (Qiagen, Hilden, Germany). Using the cDNA as input material and the Rotor Gene qPCR probe kit (Qiagen, Hilden, Germany), the transcript levels of a panel of genes associated with DNA damage and uracil metabolism (hUNG, APE1, Polβ, LigIII, DUT, SAMHD1, p53, TDG, SMUG1, MLH1, MSH2, MSH6, BRCA1, BRCA2, A3B, TS, TP, DPD) were measured relative to 18S ribosomal subunit. Thermal cycling conditions for qPCR consisted of 95 °C for 5 min, and 40 cycles of denaturation at 95 °C for 10 sec and annealing and extension at 60 °C for 30 sec.

Targeted shRNA protein depletion. Sequences for shRNA guides targeting TDG as well as a non-targeting control were synthesized by IDT (Coralville, IA) and inserted into the G418 resistant pLKO.1 plasmid from Addgene (Watertown, MA). Sanger sequencing confirmed the correct products. The pLKO.1 G418 plasmid was then transfected into T293-FT cells along with helper plasmids pspax2 and pmd2.g and virus was harvested and titered as described above. These lentiviral particles were used to infect HT29 and DLD1 cell lines. Efficient TDG knockdown was confirmed by western blot.

CRISPR Knock-out of TDG. Two independent guides targeting TDG were synthesized by IDT (Coralville, IA) and inserted into the lentiviral CRISPR cas9 plasmid from Addgene (Watertown, MA). Sanger sequencing confirmed the correct products. The lentiviral CRISPR cas9 plasmids were then transfected into T293-FT cells along with helper plasmids pspax2 and pmd2.g and virus was harvested and titered as described above. These lentiviral particles were used to infect the DLD1^{UGI} cell line. After allowing two weeks for incorporation and in-dels to form, cells were diluted into media and partitioned into 96 well plates with a calculated concentration of one cell per 3 wells. Wells were monitored and wells containing single cell colonies marked, allowed to grow to 50% confluency prior to splitting in half to allow part of the population to be sequenced to determine the presence of a homozygous in-del of TDG while the other portion

Molecular Pharmacology Fast Forward. Published on April 1, 2021 as DOI: 10.1124/molpharm.120.000191
This article has not been copyedited and formatted. The final version may differ from this version.

underwent continued proliferation. An independent clone derived from in-dels from each respective guide were identified and complete loss of protein expression confirmed by western blot.

Uracil DNA glycosylase activity in cell extracts. All cell lines containing the CW57.1 UGI construct were plated at a density of 3 x 10^5 cells per T25 flask and grown to 80% confluency in either tetracycline-free (Tet-free) media (Gibco, Gaithersburg, MD, Cat:A4736401) or media containing 0.5 μg/mL doxycycline (Tocris, Bristol, United Kingdom). Unmodified parental cells were also grown to 80% confluency in Tet-free media. Cell extracts were obtaining under native conditions by dissociating cells from the flask surface using trypsin 0.05%. Cells were then pelleted and washed x 3 with PBS. Cell pellets were then resuspended in 100 μL cell lytic M (Sigma-Aldrich, St. Louis, MO). Cells were then incubated at 4 °C for 30 minutes to allow for cell lysis. This solution was then centrifuged at 21,000 g for 20 minutes. Seventy-five microliters of supernatant was then removed and centrifuged at 21,000 g for 5 minutes. Fifty microliters was removed for use in downstream assays and protein concentrations determined using the Bradford colorimetric protein assay with bovine serum albumin (BSA) as the standard (ThermoFisher, Waltham, MA).

The total hUNG activity present in the cell extracts (the sum of the mitochondrial hUNG1 and nuclear hUNG enzymes) was measured using a 5′-FAM labeled 19mer ssDNA substrate containing a single U base pair (5′- FAM-CAC TGC TCA **dU** GT ACA GAG C-3')(Grogan *et al.*, 2011). The specificity for hUNG was confirmed by addition of uracil DNA glycosylase inhibitor protein (UGI) to the extracts, which completely abolished all uracil excision activity. Four micrograms of each extract was added to a 20 μL reaction solution containing 250 nM of the 19 mer substrate and a buffer consisting of Hepes, EDTA, Brij-35, DTT and incubated for 30 minutes. Reactions were then quenched by the addition of 2 μL of 0.2 M NaOH and heated at 90 °C for 30 min to cleave the base labile abasic sites produced by hUNG2 uracil excision. The

Molecular Pharmacology Fast Forward. Published on April 1, 2021 as DOI: 10.1124/molpharm.120.000191
This article has not been copyedited and formatted. The final version may differ from this version.

9 mer FAM-labeled product was resolved from the substrate by electrophoresis through a 15% urea denaturing polyacrylamide gel (ThermoFisher, Waltham, MA). A similar procedure was used to measure the activity of purified hUNG catalytic domain (84-304) using substrates containing FdU or BrdU (5′- FAM-CAC TGC TCA **FdU** GT ACA GAG C-3' and 5′- FAM-CAC TGC TCA **BrdU** GT ACA GAG C-3') (**Supplemental Table 3**). In this case, purified hUNG catalytic domain (2.5 nM) was added to 250 nM of the FdU or BrdU substrates. Reaction time points were taken at 10, 30 and 60 minutes and processed as described above for the cell extract measurements. The fraction of the substrate converted to product at each time point was quantified by fluorescence imaging.

Western blotting. Extracts for western blotting were prepared using denaturing conditions with approximately four million cells collected from culture plates by treatment with trypsin. To extract protein, the PBS was aspirated and the cell pellets were resuspended in cell lytic solution (Sigma-Aldrich St. Louis, MO). The resuspended pellets were incubated for 30 min at 4 °C, then centrifuged for 20 minutes at 21,000 g at 4 °C in a tabletop centrifuge. The supernatant was harvested and protein concentrations were determined using the Bradford assay with BSA as the standard. Equal amounts of protein extract were loaded in each lane of a 4-12% Bis-Tris SDS-denaturing polyacrylamide gel (Thermo) that was pre-run at 180 V for approximately 20 minutes. The loaded gel was run for 20 minutes at 60 V, followed by 40 minutes at 180 V. The gel was then transferred to a PVDF transfer membrane (Thermo) using a Thermo Scientific Pierce Power Blot Cassette at 25 V, 2.5 A for 7 minutes. The membranes were washed with blocking reagent (TBS-T + 10% milk) for 30 minutes at room temperature, followed by incubation with a 1:1000 dilution of rabbit monoclonal anti-human TDG antibody (Abcam, ab154192, Branford, CT) or anti-human TP53 antibody (Abcam, Cambridge, United Kingdom, ab1101) in TBS-T + 5% milk overnight at 4 °C.(Chen *et al.*, 2005) Following incubation with the primary antibody, the membrane was washed for 5 minutes in TBS-T buffer at room

Molecular Pharmacology Fast Forward. Published on April 1, 2021 as DOI: 10.1124/molpharm.120.000191
This article has not been copyedited and formatted. The final version may differ from this version.

temperature four times, then incubated with a 1:5000 dilution of HRP-conjugated goat anti-rabbit antibody (Abcam, Cambridge, United Kingdom, ab205718) or goat-anti-mouse antibody (Abcam, Cambridge, United Kingdom, ab205719) as dictated by the primary antibody in TBS-T + 5% milk for 1 hour at room temperature. Following incubation with the secondary antibody, the membrane was washed for 20 minutes in TBS-T at room temperature, followed by two 5 minutes washes in TBS-T at room temperature and two 5 min washes in TBS at room temperature. Membranes were treated with 1:1 solution of peroxide solution and enhancer reagent from Thermo Scientific SuperSignal West Femto and imaged for 10 to 40 secs using a Syngene G Box chemiluminescence imager (Syngene, Cambridge, United Kingdom) using a pre-optimized protocol for this reagent.

FdU concentration-response studies. Cells were grown to 50% confluence in T25 flasks prior to addition of trypsin 0.05% to detach the adherent cells. Cells were then split into two T25 flasks, one of which contained media with Tet free FBS while the other contained media with 0.5 µg/mL doxycycline. Following 48 hours growth cells were detached using trypsin and passed through a 35 µm filter (ThermoFisher, Waltham, MA) to eliminate cell clumps prior to counting with a hemacytometer. Ninety-six well plates were then seeded at a density of 2000 cells per well with the top half of each plate containing the cells grown in Tet-free conditions (hUNG proficient), and the bottom half containing cells grown with doxycycline containing media (hUNG inhibited). After 24 hours, cells cultures (in triplicate) were exposed to phenol-red free growth media containing 90 fM to 100 µM FdU in log 3 increments. For the induced cell group, doxycycline was included in the media at 0.5 µg/mL for the entire period of drug treatment. Cells were incubated in a humidified incubator for a total of 72 hours. Following this period, 10 µL of CellTiter 96 Aqueous MTS reagent and phenazine ethosulfate solution (Promega, Madison, WI) was added to each well. Absorption measurements were made at 492 nm using a Tecan Model M200 Pro plate reader (Tecan, Mannedorf, Switzerland) at 30, 60, and 120

Molecular Pharmacology Fast Forward. Published on April 1, 2021 as DOI: 10.1124/molpharm.120.000191
This article has not been copyedited and formatted. The final version may differ from this version.

minutes after addition of the MTS assay reagents. The concentration-response data in the absence and presence of hUNG activity were fitted to eq 1 using Graphpad prism software, where C is an offset, A is the total amplitude for the loss in cell viability, EC_{50} is the drug concentration where one-half of the total viability loss occurs, X is the drug concentration and *n* is the Hill slope parameter.

$$\% \text{ viable cells} = C + [A/(1 + 10^{[\log (EC50 - [X])*n]}] \quad (1)$$

Cell proliferation measurements. To confirm the MTS assay results we also investigated the effects of FdU and FU on proliferation of the DLD1 (R) and SW620 (NR) cell lines using an Incucyte ZOOM cell imaging system. For these experiments, DLD1 and SW620 cells were grown to 50% confluence in T25 flasks prior to addition of trypsin 0.05% to detach adherent cells. Cells were then split into two T25 flasks, one of which contained media with Tet free FBS while the other contained media with 0.5 µg/mL doxycycline. Following 48 hours growth, cells were detached using trypsin and passed through a 35 µm filter (ThermoFisher, Waltham, MA) to eliminate cell clumps prior to counting with a hemacytometer. Cells were plated in 24 well plates at 500 cells per well. After allowing 24 hours for adherence and recovery, cells were exposed to FdU across a range of concentrations (0.26 nm to 4000 nM for DLD1 and 0.03 to 500 nM for SW620) in technical duplicates. Cells were then placed into the Incucyte ZOOM system with confluence of each well measured every 8 hours for a total of 72 hours. Cellular confluence for each cell line at a given FdU concentration was plotted as a function of time for both the UNG active and inhibited states. The confluence of each cell line at 72 hours was also plotted as a function of FdU concentration evaluated in both the UNG active and inhibited states. Measurements were obtained in biological duplicate each with two technical replicate wells.

Nucleoside rescue of drug toxicities. HT29 and DLD1 cell lines were grown in Tet-free or doxycycline containing media for 48 hours prior to plating at 2000 cells per well in 96 well plates. After 24 hours, cells were exposed to 41 pM to 16 µM FdU (log 5 dilutions) or 180 pM to 1.2 µM

Molecular Pharmacology Fast Forward. Published on April 1, 2021 as DOI: 10.1124/molpharm.120.000191
This article has not been copyedited and formatted. The final version may differ from this version.

RTX (log 3 dilutions) in media that was supplemented with 100 μM concentrations of dU, or dT. Plates were incubated for 72 hours. The MTS assay and data fitting were performed as described above.

Structure activity studies using 5-substituted deoxyuridine analogues. Cell lines were grown under Tet-free or doxycycline-exposed conditions and plated at 2000 cells per well in 96 well plates as described in the FdU concentration-response methods above. After 24 hours, cell cultures (in triplicate) were exposed to phenol-red free growth media containing either BrdU (256 nM to 100 μM), or dU (26 nM to 10 mM) using log 5 dilutions. For the induced cell group, doxycycline was included in the media at 0.5 μg/mL for the entire period of nucleoside treatment. Cells were cultured in a humidified incubator for 72 hours. The MTS assay and data fitting were performed as described above.

U and FU DNA incorporation measurements by LC/MS. Representative FdU responsive (DLD1^{UGI} and HT29 ^{UGI}) and nonresponsive (SW620 ^{UGI} and LoVo ^{UGI}) cancer cell lines were each plated into 4-T75 flasks at 2 x 10^6 cells per flask. Two of these 4 flasks were plated into RPMI supplemented with 10% Tet-free FBS while the other two were grown in RPMI supplemented with 10% FBS containing 0.5 μg/mL doxycycline. After allowing 48 hours for cellular adherence and UGI expression, cells were switched to RPMI media without any serum present. Doxycycline supplementation was continued if previously present. Cells were maintained in serum-free RPMI media for 48 hours to allow G1 cell cycle arrest. Cells were then switched to full growth media for 2 hours to restore nucleotide pools followed by one of four conditions: i) full growth media, ii) doxycycline containing media, iii) full growth media containing 5 μM FdU, and iv) media containing 5 μM FdU and doxycycline. After 24 hours, cells were washed with PBS and dissociated with 0.05% trypsin. Following detachment, cells were centrifuged at 400 g x 10 minutes to pellet followed by two PBS washes. Genomic DNA was extracted using the NEB Monarch Genomic DNA purification kit (NEB, Ipswich, MA) and

Molecular Pharmacology Fast Forward. Published on April 1, 2021 as DOI: 10.1124/molpharm.120.000191
This article has not been copyedited and formatted. The final version may differ from this version.

performed using the protocol provided by NEB. DNA was eluted from the column with 50 µL of DNase free water heated to 56 ^{o}C. A typical extracted DNA yield from 1.7 x 10^7 cells was ~200 µg. To avoid column overloading, no more DNA than obtained from 5 x 10^6 cells was used. DNA concentrations were calculated using A^{260} values obtained from NanoDrop spectrophotometer measurements (Thermofisher, Walham, MA).

To avoid accumulation of salt and buffering agents during lyophilization a volatile buffer of *N*′,*N*-ethylmorpholine, adjusted to pH 8.0 with glacial acetic acid (Sigma), was used during the enzymatic excision of U and FU. DNA samples (100-400 µg of DNA) were supplemented with *N*′,*N*-ethylmorpholine acetate to yield a final buffer concentration of 20 mM in a final volume of 500 µL. Purified human UNG enzyme was added to a final concentration of 100 nM and incubated overnight at room temperature. At the end of the overnight incubation, heavy labeled (^{15}N, ^{13}C) uracil and fluorouracil (Cambridge isotopes, Tewksbury, MA) were spiked to a final concentration of 200 nM each. Heavy isotope standards are dissolved in water, and their concentrations were determined using their respective extinction coefficients for U (8,200 cm^{-1} M^{-1} at 258 nm) and FU (7,070 cm^{-1} M^{-1} at 265 nm). To remove DNA and enzyme from the excised U/FU nucleobases, each sample (500 µL) was spun through a 3 kDa Amicon mini-concentrator membrane (0.5 mL capacity). When the membrane has reached the dead volume, 0.4 mL of 60% MeOH was added to wash residual U/FU from the membrane. The two fractions are combined, frozen, and lyophilized overnight. Dry residues were dissolved in 50 µL of nuclease free water, vortexed and spun at 17000 x g for 20 minutes to remove any small particulates and transferred to a 96-well plate for HPLC/MS analysis. These identical procedures were repeated for two representative R cell lines (HT29, DLD1) across the same treatment conditions i) full growth media, ii) doxycycline containing media, iii) full growth media containing 5 µM FdU, and iv) media containing 5 µM FdU and doxycycline in media supplemented with either 100 µM dT or 100 µM dU.

Molecular Pharmacology Fast Forward. Published on April 1, 2021 as DOI: 10.1124/molpharm.120.000191
This article has not been copyedited and formatted. The final version may differ from this version.

LC/MS analysis. The supernatants were collected after centrifugation at 21,000 g and 10 µL was directly injected onto a Hypercarb column (Thermofisher, Walham, MA, 35003-10230, 100 x 2.1 mm, 3-micron pore size) equilibrated in 100% buffer A (0.1 % formic acid in water buffer; buffer B is 100% acetonitrile). An Agilent 1290 Infinity II HPLC system was used for separation with a gradient of 0-18% B from 0-2.75 minutes, and 18-100% B from 2.75-3 minutes, and then 100% B from 3-4 minutes before returning to 100% A for a total of 3 minutes to re-equilibrate before subsequent sample injections (10 µL). This method allows for facile separation of U from FU. Detection of substrates and products was performed by electrospray ionization in negative mode (ESI-) using an Agilent Triple Quadrupole (6495) mass spectrometer. Identification of each analyte was carried out using a MRM method according to **Supplemental Table S4**. To quantify the amount of U or FU in picomoles, the ratiometric difference between the analytes and their respective $^{13}C^{15}N$ internal standards was used. In addition, we used a standard curve with concentrations ranging from 10 fmol – 10 pmol. Results from either method showed less than 2% difference. The number of U or FU bases per million bases of diploid genomic DNA was then calculated.

Statistics. Data were analyzed using the Prism 8.0 statistical program from GraphPad Software. The uncertainties in the IC_{50} values derived from the concentration-response curves for FdU are expressed as the mean ± 1 standard deviation and are derived from at least three biological replicates, each performed with three technical replicates. The uncertainties in the concentration-response curves for FU and RTX were obtained from two biological replicates, each performed with three technical replicates. Pairwise statistical analysis of test groups was performed by a two-tailed unpaired Student's *t*-test, assuming equal variances between groups. Due to the exploratory character of the work the calculated *p*-values cannot be interpreted as hypothesis-testing.

Molecular Pharmacology Fast Forward. Published on April 1, 2021 as DOI: 10.1124/molpharm.120.000191
This article has not been copyedited and formatted. The final version may differ from this version.

RESULTS

Inducible overexpression of UGI abolishes hUNG activity in a panel of cancer cell lines

The CW57.1 lentiviral construct carrying the doxycycline inducible uracil DNA glycosylase inhibitor protein (UGI) was introduced into 21 cancer cell lines originating from colon, breast, gastric, hepatocellular, pancreas and lung tumors. This panel also included the HCT116 colorectal line and its engineered isogenic TP53 knock-out (**Supplemental Fig. S1**). Following selection with puromycin for one-week, cellular lysates were prepared from these cells grown either in either tetracycline-free media or media containing 0.5 μg/mL doxycycline to induce UGI expression. The UNG activity present in each extract was then measured using a 5'-FAM labeled ssDNA 19mer substrate containing a central uracil residue. hUNG excision of the uracil gives rise to a 5'-FAM labeled 9mer ssDNA product after treatment with base and heat, which is resolved from the substrate by denaturing polyacrylamide gel electrophoresis (**Fig. 2A**). All parental cell lines and their UGI-transduced derivatives in the absence of induction showed readily detectable UNG activity after 30 min reaction using 4 μg of each cell protein extract. In contrast, the UGI transduced cells grown in the presence of doxycycline had no measurable product formation under identical conditions (**Fig. 2A,** non-colorectal lines are in **Supplemental Figure S2**). These activity measurements established the presence of robust hUNG activity in the absence of UGI induction and complete inhibition after the addition of doxycycline. The persistent inducible inhibition of hUNG by UGI was confirmed over the time span of the experiments (**Supplemental Figure S3**).

hUNG inhibition enhances potency of FdU for over one-half of colon cancer cell lines tested

All 21 cell lines were exposed to FdU across a broad range of concentrations in the presence and absence of UGI induction to ablate hUNG activity. Cell survival was then assessed using the MTS colorimetric viability assay. The concentration-response curves for 12 colorectal lines

Molecular Pharmacology Fast Forward. Published on April 1, 2021 as DOI: 10.1124/molpharm.120.000191
This article has not been copyedited and formatted. The final version may differ from this version.

are shown in **Fig. 2B** and **2C** (the concentration-response curves for the other lines are shown in **Supplemental Fig. S4**). Fitting these concentration-responses to eq 1 showed that the FdU IC_{50} values for six colorectal cell lines decreased by 6 to 70-fold following hUNG inhibition (HT29, SW480, KM12, DLD1, HCT15, HCT116) (**Fig. 2B**), while the responses of the remaining five lines and the isogenic HCT116 TP53 knock-out were unaffected by hUNG activity (Colo205, HCC2998, HCT116 TP53, LoVo, LS513, SW620) (**Fig. 2C**). In addition to these colorectal lines, one breast cancer line (MCF7, $p53^{wt}$) was significantly sensitized by inhibition of hUNG activity (**Fig. S4**). Although the hUNG responsive colorectal lines ("responders, R") were enriched in TP53 mutant phenotypes (five out of six), this trend was reversed for $p53^{wt}$ HCT116 (R) parent line and its isogenic $p53^{mut}$ form ("non-responder, NR"), as well as the highly responsive MCF7 $p53^{wt}$ breast cancer line (**Fig. S4**). Although it has been previously suggested that TP53 mutant status might be a useful biomarker for the R phenotype, six out of nine of the other tumor lines tested were TP53 mutant but NR phenotypically, further indicating that p53 status alone is not a reliable predictor across all cancers (Yan *et al.*, 2018). This broad data set indicates that hUNG excision of U or FU bases in DNA is not required for FdU efficacy, regardless of p53 activity. Moreover, in a subset of the cell lines the inhibition of hUNG sensitizes cells that would otherwise be FdU resistant.

To investigate whether the R and NR phenotypes were related to differential expression of DNA damage response or uracil metabolism gene products, we tested the expression levels of 15 these genes by RT-PCR, but no obvious expression differences were observed **(Supplementary Fig. S5)**. We also evaluated whether representative R and NR cell lines followed an apoptotic mechanism of cell death using annexin V staining and flow cytometry. For both R and NR lines [HT29, HCT116 ($TP53^{wt}$), DLD1, SW620, HCT116 ($TP53^{KO}$), Lovo] increased annexin V staining was observed when the cells were treated with 100 nM FdU continuously for 72 h **(Supplementary Fig. S6, S7)**. When hUNG was inhibited, these same

Molecular Pharmacology Fast Forward. Published on April 1, 2021 as DOI: 10.1124/molpharm.120.000191
This article has not been copyedited and formatted. The final version may differ from this version.

lines showed a two to four-fold increase in annexin V staining compared to that when hUNG activity was present. Consistent with previous findings, these data indicate that FdU induces apoptosis and that hUNG inhibition potentiates this outcome.(Weeks *et al.*, 2014; Huehls *et al.*, 2016; Yan *et al.*, 2016) In addition, we observed that the effect of hUNG inhibition was much greater in the TP53 knock-out HCT116 line compared to its parental line with a functional TP53 gene (**Fig. S6**). This result suggests that TP53 activity is not an absolute requirement for an FdU apoptotic response.

Finally, previous work by the Gerson and Karnitz groups has established that FdU induces DNA strand breaks and replication fork stalling, which are the precipitating factors for the observed apoptotic response.(Huehls *et al.*, 2016; Yan *et al.*, 2016) We confirmed this by probing for histone γH2A.X levels in the presence of 48 h continuous exposure to 1 μM FdU using the DLD1 and SW620 cell lines. Notably, in the absence of hUNG, a large increase in γH2A.X were observed in Western blots of extracts prepared from both cell lines (**Fig. S6C, D**). The apoptotic response was independent of caspase cleavage and activation because inclusion of the pan-caspase inhibitor Ac-DEVD-CHO did not affect the observed increases in histone gH2A.X (**Fig. S6E**). Caspase independent apoptosis has been previously indicated for pemetrexed in studies by the Gerson group.(Weeks *et al.*, 2014; Yan *et al.*, 2016, Bulgar et al., 2012)

FU toxicity does not require hUNG excision

Given the major role of FU in treatment of colorectal cancer, we next asked whether the same hUNG R phenotype would be manifested with FU. This question was addressed using the same six hUNG responsive colorectal lines revealed in the concentration-response studies with FdU above. In stark contrast to FdU, none of these previously responsive lines showed any significant response to hUNG inhibition in the context of FU treatment (**Fig. 2D and Supplemental Table S5**). This is consistent with previous reports that FU toxicity arises

Molecular Pharmacology Fast Forward. Published on April 1, 2021 as DOI: 10.1124/molpharm.120.000191
This article has not been copyedited and formatted. The final version may differ from this version.

primarily from the RNA pathway, even though dTMP levels are diminished and FU and U bases can be detected in DNA upon treatment with this drug (Mojardín *et al.*, 2013). The present results require that any FU toxicity arising from the DNA pathway cannot involve cytotoxic levels of U or FU incorporated into DNA because responsiveness to hUNG inhibition should have been observed. However, a contribution from the DNA pathway arising from FU-mediated thymidine depletion is possible.

We further investigated whether the R and NR phenotypes obseved with FdU and FU persisted in a cell proliferation assay, rather than the MTS assay which uses a metabolic marker (**Supplemental Figure S8**). DLD1 (responsive) and SW620 (non-responsive) cells were incubated under hUNG proficient and inhibited conditions and exposed to a range of FdU concentrations. Cellular confluence was then measured using an Incucyte ZOOM live-cell imaging system over the course of 72 hours to match the drug exposure time in the MTS assay. These measurements demonstrated a 5-fold increase in FdU sensitivity in the responsive DLD1 cell line under hUNG inhibited conditions and no substantial shift in sensitivity for the non-responsive SW620 cell line. Of note, the difference in confluence for the DLD1 cell line in the hUNG proficient and inhibited states only became apparent after 48 hours of drug exposure suggesting that incorporated U and FU bases only become toxic after a second round of DNA replication.

FU and U levels in genomic DNA in responsive (R) and non-responsive (NR) cells

We were interested in whether the differences between the hUNG R and NR cell types might be related to different levels of U and FU incorporated into DNA in these lines and the persistence of these bases in the absence of hUNG activity. One major experimental challenge in answering this question quantitatively is that R and NR cell types have very different IC_{50} values for FdU, different growth rates and rates of progression through the cell cycle, and very different responses to hUNG inhibition. To at least partially control for these differences and to provide a

Molecular Pharmacology Fast Forward. Published on April 1, 2021 as DOI: 10.1124/molpharm.120.000191
This article has not been copyedited and formatted. The final version may differ from this version.

constant reference state for evaluating two representative responsive (R) and non-responsive (NR) lines, we decided to use an approach where cells were cultured under serum starvation to arrest at the G1/S border for 48 hours. Following arrest and synchronization, the cells were released into regular media for two hours to restore nucleotide levels before addition of 5 μM FdU. The cells were then cultured for another 24 h to allow for nucleotide incorporation and progression through S phase. The genomic DNA was isolated and assessed for the FU and U content using LC/MS.

Across the four cell lines evaluated, there was a significant increase in genomic FU when cells were exposed to FdU, which were further increased upon inhibiton of hUNG. There were several notable trends in the data. First, inhibition of hUNG in combination with FdU treatment had a greater effect on genomic FU levels as compared to U (**Fig. 3A, 3B**). Second, large differences in genomic U levels between cell lines were observed in the absence of drug with hUNG inhibition (**Fig. 3A)**. In particular, the SW620 (NR) line showed ~10-fold higher U content than the HT29 (R) cell line. In contrast, upon treatment with FdU and hUNG inhibition, all four lines were more similar with respect to their genomic U and FU levels. We performed quantitative rate measurements of hUNG catalyzed U excision using extracts from all of these lines and found no correlation between cellular responsiveness and their baseline hUNG activity (**Supplemental Fig. S9**). In conclusion, there is no evidence that differences in genomic U and FU levels in the R or NR phenotypic lines, or different hUNG activities, accounts for their different respsonses to hUNG inhibition.

Evaluating contributions of thymidine depletion and dU incorporation using raltitrexed (RTX)

A complexity with determining the toxicity mechanisms of FU and FdU with respect to the DNA pathway is that these agents result in multiple effects that include thymidine depletion as well as elevated dUTP and FdUTP (**Fig. 1A**). One strategy to evaluate the effects of dUTP and

Molecular Pharmacology Fast Forward. Published on April 1, 2021 as DOI: 10.1124/molpharm.120.000191
This article has not been copyedited and formatted. The final version may differ from this version.

thymidine depletion in isolation is to use the highly specific thymidylate synthetase inhibitor raltitrexed (RTX)(Van Cutsem *et al.*, 2002). We have previously shown that this drug dramatically increases the dUTP/dTTP ratio and results in uracil bases in DNA (Grogan *et al.*, 2011; Weil *et al.*, 2013). Thus, we treated our entire panel of R and NR colorectal cell lines to a range of RTX concentrations in the presence and absence of hUNG inhibition (**Fig. 4**). Unlike the findings for FdU, these experiments demonstrated no significant shift in IC_{50} values for RTX upon hUNG inhibition (**Supplemental Table S6**). However, as noted in the next section there was a reduction in viability upon hUNG inhibition as measured by an area under the curve (AUC) analysis that was larger for the responder group (26% reduction versus 8% for the non-responder group). Since inhibition of hUNG would not affect the thymidine depletion component, the extra sensitization arising from hUNG inhibition in the R lines may arise from the persistence of uracil in DNA under conditions of thymidine depletion. The minor effects of hUNG inhibition with RTX suggests that the large effects of hUNG inhibition observed with FdU arise from the unique properties of persistent FU bases or the cellular response to FU bases in DNA (see Discussion).

The relative effects of hUNG inhibition on cell killing by FdU, FU and RTX are shown in **Figure 5** for all of the hUNG R and NR colon cancer lines. To best capture the total cell killing effect, the AUC values for RTX are compared rather than the IC_{50} values (Kaldate *et al.*, 2012). For FdU, there is a clear demarcation between the IC_{50} values for the R and NR lines when hUNG is active (black data, **Fig. 5A**)(p = 0.0019), but when it is inhibited, the differences between these groups disappears (red data, **Fig. 5A**). In the case of FU, the two groups are indistinguishable based on their IC_{50} values (**Fig. 5B**), and for RTX, a modest segregation of the two groups is observed based on AUC)(p = 0.05), but not IC_{50} values (**Fig. 5C)**. Thus, using hUNG responsiveness as a criiterion of mechanism, FdU toxicity is unique in its sensitivity to hUNG inhibition (**Fig. 1a**).

Molecular Pharmacology Fast Forward. Published on April 1, 2021 as DOI: 10.1124/molpharm.120.000191
This article has not been copyedited and formatted. The final version may differ from this version.

Evaluating the role of FU/A, U/A, and FU/G base pairs in toxicity of FdU

FU, and to a much lesser extent U, have a greater propensity to form mispairs with G as compared to T due to their lower imino proton pK_a values and altered tautomeric equilibria (Sowers *et al.*, 1988). Indeed, FdUTP is incorporated by human replicative DNA polymerases with nearly equal frequency opposite to A and G in the template strand, while dUTP and dTTP greatly favor pairing with A (Meyers *et al.*, 2005). Thus, significant levels of two toxic base pairs may be formed during treatment with FdU: FU/A and FU/G.

To explore the impact of these two base pairs we exposed cells to FdU in the presence and absence of hUNG inhibition while supplementing the media with either 100 μM dT or dU. The logic behind dT supplementation is that thymidine depletion is prevented and incorporation of FU or U opposite to A will be out competed by the higher concentration of dTTP in the nucleotide pool. In contrast, dTTP is not expected to compete efficiently with FdUTP for base pairing with G. In the case of dU supplementation, its metabolite dUMP is expected to directly compete with FdUMP for binding to TS (**Fig. 1A**), and since dUMP is the substrate for TS, this will lead to increased dTMP levels as compared to treatment with FdU alone (Sommer and Santi, 1974; Myers *et al.*, 1975). Thus in the presence of dU supplementation, the relative levels of dTTP precursors will be increased relative to no supplementation, but in addition, the triphosphate form of dU can also be incorporated into DNA in the form of U/A base pairs (Myers *et al.*, 1975; Weil *et al.*, 2013).

The effects of dT supplementation in conjunction with FdU dosing are consistent with the above suggested mechanisms. First, we confirmed that dT and dU supplementation led to the expected changes with respect to FU and U levels in DNA using the LC/MS method described above (**Fig. 6A**). Supplementation with dT increased the IC_{50} values for FdU in HT29 and DLD1 responsive cells by two to four log units, with the largest increases being observed under the condition of hUNG inhibition (**Fig. 6B, C)**. Importantly, dT supplementation completely

Molecular Pharmacology Fast Forward. Published on April 1, 2021 as DOI: 10.1124/molpharm.120.000191
This article has not been copyedited and formatted. The final version may differ from this version.

eliminated the responsiveness to hUNG inhibition that was observed with FdU alone (dashed lines **Fig. 6B**). The observation that dT abrogates the responsive phenotype and dramatically depletes the number of U and FU bases in DNA (**Fig. 6A**), indicates that persistent FU bases in the absence of UNG activity is one major origin of responsiveness (findings below establish that U bases are non-toxic in the absence of thymidine depletion). Although the protective effect of 100 μM dT was diminished as the FdU concentration neared similar levels (**Fig. 6B**), this is almost certainly due to direct competition of FdUTP with dTTP for incorporation into DNA. Thus, this data indicates that 100 μM dT completely rescues the toxic effects of lower cytotoxic concentrations of FdU.

Supplementation with a non-toxic (see below) 100 μM concentration of dU during dosing with FdU increased the FdU IC_{50} values for the responsive HT29 and DLD1 lines, but by about one log unit less than observed with dT supplementation. Unlike dT supplementation, the cell line responsiveness to hUNG inhibition persisted in the presence of dU (**Fig. 6C**). The increase in the IC_{50} values for FdU in the presence of dU can be attributed to two possible mechanisms (i) efficient conversion of dU into dUMP which partially competes with FdUMP for binding to TS, leading to increased dTTP levels, and (ii) competition between dUTP and FdUTP for incorporation opposite to template adenines (dUTP incorporation using 100 μM dU is non-toxic by itself and does not show any UNG responsiveness; see below).

The effects of dT and dU supplementation during dosing with RTX support the above conclusion that FU/A (and FU/G) base pairs, but not U/A, are the major toxic lesions produced by FdU. Supplementation with dT completely rescued the toxic effect of RTX, which is expected given that the dTTP pool is restored by bypassing the inhibited TS enzyme (**Fig. 6B**). Supplementation with dU did not change the IC_{50} or cytoxicity of RTX (**Fig. 6C**), which is consistent with fact that RTX binds to the folate binding site of TS, and thus, dTTP pools remain depleted even though dUMP levels are high. Since 100 μM dU is non-toxic on its own (see

Molecular Pharmacology Fast Forward. Published on April 1, 2021 as DOI: 10.1124/molpharm.120.000191
This article has not been copyedited and formatted. The final version may differ from this version.

below), the toxic effects of RTX must be mostly attributed to thymidine pool depletion rather than introduction of dU into DNA.

Finally, supplementation with dT or dU in the context of FU dosing had no effect on the concentration-response curves for the DLD1 line and only small effects for the HT29 line (**Fig. 6B, C**). Although dU supplementation did shift the IC50 curves rightward for the HT29 line, there were only ~2-fold changes in fractional cell killing at any concentration of FU due to the broad concentration-response observed with FU alone. Once again, an RNA pathway is strongly indicated for FU, but the HT29 cell line may also have a minor DNA pathway component for FU (**Fig. 1A**).

In summary, the supplementation data indicate that the increased FdU toxicity in cell lines that show responsiveness to hUNG inhibition at least partly results from the persistence of FU/A pairs which can be effectively rescued by dT or dU supplementation. In addition, persistent FU/G pairs are also likely to be important. In contrast, a toxic role for persistent U/A pairs is not indicated because 100 μM dU is completely nontoxic on its own, both in the absence and presence of hUNG activity (see below), and dU supplementation substantially abrogates the cytoxicity of FdU (**Fig. 6C**). Thus, in the case of RTX, the toxicity arises primarliy from thymidine starvation rather than U/A pairs, and accordingly, RTX toxicity is fully rescued by dT. The above interpretations of nucleoside supplementation effects are strongly supported by (i) previously measured changes in dTTP, dUTP and FdUTP concentrations in HT29 cells upon treatment with FU, FdU and RTX, (ii) measurements of FU and U levels in genomic DNA reported above, and (iii) the relative activity of hUNG on U and FU containing DNA substrates (see below)(Grogan *et al.*, 2011; Weil *et al.*, 2013).

hUNG responsiveness does not extend to deoxyuridine (dU) and bromodeoxyuridine (BrdU)

Molecular Pharmacology Fast Forward. Published on April 1, 2021 as DOI: 10.1124/molpharm.120.000191
This article has not been copyedited and formatted. The final version may differ from this version.

Since the toxicity of FdU in responder cells was determined by hUNG activity, we were curious whether the toxicity of other deoxyuridine analgoues (dU, BrdU) might correlate with the ability (or inability) of hUNG to excise these bases in the context of DNA. To assess this, we synthesized a series of 19mer 5′-FAM labeled ssDNA substrates that contained a single centrally located U, FU or BrU base (**Fig. 7A**). The substrates were reacted with hUNG catalytic domain and the reaction products were processed and analyzed by gel electrophoresis as described in **Figure 2A** and the Methods. The kinetic timecourses for these substrates revealed that dU was excised 30-times faster than FU, and that excision of BrU was undetectable. **(Fig. 7A)**. These results impact interpretation of the FdU toxicity mechanism because the poor reactivity of FU indicates that it is more likely to persist in DNA after incorporation even when hUNG activity is present (see Discussion).

We dosed the HT29^{UGI} and DLD1^{UGI} cell lines with dU and BrdU nucleosides for 72 hours and determined cell viability using the MTS assay **(Fig. 7B).** Surprisingly, dU was remarkably non-toxic to both lines with IC_{50} values of almost 10 mM. In addition, there was no responsiveness to UNG inhibition despite uracil being a preferred substrate in DNA. In contrast, BrdU was toxic at concentrations 100-fold lower than dU with no responsiveness to hUNG inhibition, as would be expected based on its inability to serve as a substrate for hUNG in the *in vitro* activity assay.

The very weak toxicity of dU is consistent with its ability to partially rescue the toxic effects of FdU (**Fig. 6B**), and the preferred reactivity of hUNG for U bases *in vitro* also suggests efficient excision in the context of genomic DNA. Thus during dosing with dU, uracil excision and generation of toxic abasic sites must occur, but these lesions must be efficiently replaced with T or U to prevent the anticipated severe effects on DNA replication and cell growth. Apparently, persistent U/A pairs are well tolerated by the cell when hUNG activity is inhibited (no other cellular DNA glycosylase readily accepts U/A pairs as a substrate)(Kavli *et al.*, 2002; Grogan *et*

Molecular Pharmacology Fast Forward. Published on April 1, 2021 as DOI: 10.1124/molpharm.120.000191
This article has not been copyedited and formatted. The final version may differ from this version.

al., 2011). We rationalize that the greater toxicity of BrdU most likely stems from its inhibition of TS and perhaps UNG-independent excision (Maley, 1962). Possibilities for excision of the BrU base include SMUG and TDG DNA glycosylases or mismatch repair, all of which have a substrate spectrum that includes BrU (and FU) if it is paired with guanine on the opposite strand (Meyers *et al.*, 2005; Morgan *et al.*, 2007).

TDG activity does not modulate FdU sensitivity following hUNG inhibition in responsive cells

Prior reports have suggested that in the absence of hUNG, TDG intervenes to mediate removal of FU/G and U/G base mismatches, which precipitates post-S phase cell cycle arrest (Fischer *et al.*, 2007; Huehls *et al.*, 2016)**.** To clarify whether the increased efficacy of FdU when UNG was inhibited in our responsive cell lines also depended on TDG, we generated TDG knock-outs (KOs) and knock-downs (KDs) using CRISPR and shRNA methodology, respectively. In the DLD1 CW57.1 UGI background, two independent KO clones were isolated after puromycin selection using different CRISPR guide sequences (**Supplementary Table 1**). These clones were validated using Sanger sequencing where homozygous frameshift mutations were confirmed (**Supplementary Figure S10**). In addition, we used shRNA methodology to generate two TDG KDs in the DLD1 and HT29 CW57.1 UGI backgrounds. For both the DLD1 KO and DLD1/HT29 KD lines, the absence or substantial reduction of TDG protein expression was confirmed by Western blot analysis (**Fig. 8A, B**). We then assessed whether TDG loss impacted sensitivity of cells to FdU under conditions where hUNG was active (black data) or inhibited (red data) (**Fig. 8C, D**). Comparisons of the concentration-response curves between the TDG KOs or KDs and the respective control or parent line indicates that TDG does not determine the hUNG responsiveness to FdU in these lines.

DISCUSSION

Molecular Pharmacology Fast Forward. Published on April 1, 2021 as DOI: 10.1124/molpharm.120.000191
This article has not been copyedited and formatted. The final version may differ from this version.

What makes a cell hUNG-responsive versus nonresponsive?

The most fundamental observation from our extensive data set is that NR lines have low IC_{50} values for FdU regardless of hUNG activity, while the R lines are resistant to FdU until hUNG activity is inhibited (**Fig. 5**). A useful distinction is to consider the possibility of pre- and post-DNA incorporation events as the basis for the differences in these lines. Possible pre-incorporation differences that could influence responsiveness include nucleoside transport, expression levels of activating kinase enzymes, or differences in pathways for degrading the FdU nucleoside (ie. thymidine phosphorylase). Post-DNA incorporation events include differences in cell cycle checkpoint proteins (chk1, p53, ATM, AKT, Wee1, etc.), DNA repair pathways, or signaling pathways promoting cell death (Geng *et al.*, 2011; Datta *et al.*, 2016; Kim *et al.*, 2016; Yan *et al.*, 2018).

The most useful measurement that includes all steps leading to and including nucleotide incorporation into DNA are the direct measurements of the U and FU levels in genomic DNA for both responsive and non-responsive lines (**Fig. 3, Fig. 6A**). Although there were differences in genomic uracil levels between the lines under basal conditions, the differences did not segregate according to responsiveness. Further, under the condition of FdU treatment, there was no indication that R or NR lines differed with respect to genomic dU or FdU, regardless of hUNG activity status. Given these incorporation results we think it is unlikely that the fundamental difference between R and NR lines resides in any of the steps upstream of nucleotide incorporation.

The simplest mechanism that could give rise to the different responsiveness of the cell lines subsequent to U or FU incorporation into DNA would be low baseline hUNG activity in the NR lines, which would make them resemble the hUNG inhibited state. However, we directly excluded this possibility by quantifying hUNG activity in cell extracts from both R and NR colorectal lines and found no correlation of activity with the R/NR phenotypes (**Supplementary**

Molecular Pharmacology Fast Forward. Published on April 1, 2021 as DOI: 10.1124/molpharm.120.000191
This article has not been copyedited and formatted. The final version may differ from this version.

Fig. S9). Of course, many other possibilities for post-incorporation differences between the R and NR lines exist, most notably, possible differences in checkpoint signaling. One post-incorporation mechanism that we directly tested was suggested by prior work of the Karnitz group (Geng *et al.*, 2011). Their results showed that when hUNG protein was ablated in the context of FU incorporation, synchronized progression through the cell cycle was slowed at the second G1/S phase transition, with markedly hindered progression through S phase and activation of homologous recombination (HR) which was dependent on TDG in the absence of hUNG (Geng *et al.*, 2011; Huehls *et al.*, 2016). In contrast, our studies did not detect a significant change in FdU cytotoxicity in the combined context of UGI inhibition and TDG CRISPR knock-out or shRNA depletion in two responder cell lines (**Fig. 8**). While we cannot rule out that TDG activity might modify FdU sensitivity in some hUNG deficient backgrounds, we found no evidence that TDG is a required mediator of FdU cellular toxicity in the absence of hUNG activity.

Finally, we also pursued an unbiased whole transcriptome search leveraging pre-existing data available through the Cancer cell line encyclopedia and performed a Gene Set Enrichment Analysis (GSEA) on the responsive and non-responsive lines (Subramanian *et al.*, 2005; Barretina *et al.*, 2012). Using 1,502 curated gene sets (compiled in the Molecular Signatures Database) that encompass a wide range of biological relevance, we looked for gene sets enriched in different paired comparisons. First, we looked at colon cancer cell lines alone, in order to control for tissue specific expression differences; second, we looked at all of our responsive and non-responsive lines, in order to increase the sample number. None of the comparisons resulted in a gene set having a false discovery rate (FDR) q-value <0.25 even though gene sets with p-values <0.01 were observed. The lack of low FDR q-values could be a result of low sample number or a subtle biological signal. Nevertheless, there were trends suggesting that expression of ion channel transporters and the NOTCH1 signaling pathway

Molecular Pharmacology Fast Forward. Published on April 1, 2021 as DOI: 10.1124/molpharm.120.000191
This article has not been copyedited and formatted. The final version may differ from this version.

might be lower in the R cell lines, resulting in resistance that was overcome by hUNG inhibition. We explored the FdU sensitivity of the DLD1 and HT29 R lines in the presence of single saturating concentrations of small molecule inhibitors of ion channel (verapamil) and NOTCH1 pathways (RIN1) under UNG-active and inhibited conditions (**Supplemental Figure S11**). These additional treatments did not ablate the R phenotypes, nor did they introduce significant or anticipated changes in the IC_{50} values.

Nature of the toxic DNA lesion

The use of FdU, FU and RTX in the context of hUNG inhibition and in conjunction with nucleoside supplementation (dT, dU, BrdU) provides insight into the relative toxicities of various DNA lesions that are generated with these nucleosides. One surprising finding was that dU was essentially nontoxic (IC_{50} ~ 10 mM), independent of hUNG inhibition, even though it is the most favored substrate (**Fig. 7**). This suggests that any dUTP incorporated in the form of U/A base pairs during RTX or FdU treatment is not intrinsically toxic, regardless of whether the uracil is excised by hUNG or persists in the absence of hUNG activity. Thus, any component of toxicity that is derived from excision from U/A pairs must also require inhibition of TS by these drugs. Without the additional component of TS inhibition (thymidine starvation), uracil excision by hUNG is counteracted by efficient replacement of U with T (or U) through base excision repair, both of which are non-toxic. In the absence of hUNG activity, intact U/A pairs are well-tolerated. A requirement for TS inhibition and thymidine depletion in the toxicity of U/A pairs is supported by the results with the TS inhibitor BrdU, which is not a substrate for hUNG, but is toxic at concentrations 100-fold lower than dU (**Fig. 7**)(Maley, 1962).

The vastly more potent toxicity of FdU as compared to BrdU or dU requires that the FdU nucleoside has unique properties unrelated to its ability to inhibit TS (like BrdU) or introduce uracil into DNA (like dU). We surmise that persistence of the FU base in DNA is a key aspect of the action of FdU in R cell lines. Persistence is strongly suggested by the increased toxicity in

Molecular Pharmacology Fast Forward. Published on April 1, 2021 as DOI: 10.1124/molpharm.120.000191
This article has not been copyedited and formatted. The final version may differ from this version.

the absence of hUNG activity. The molecular mechanism is most likely related to the electronic properties of the FU base. It is well established that FU exists in a pH dependent equilibrium between a wobble and ionized base pair anion while pairing with G (Sowers *et al.*, 1988; Parker and Stivers, 2011). This property of FU is attributed to the electron withdrawing fluorine atom which lowers the pK_a value of the N3 imino proton (pK_a = 8.3), increasing the likelihood that this base will be misincorporated opposite to G by replicative DNA polymerases. Studies performed with mismatch repair deficient HCT116 human colon cancer cells demonstrated that ~50% of the genomic 5-FU was incorporated opposite to guanine (Meyers *et al.*, 2005). Further, the anion form of the FU base is problematic for excision by UNG because cleavage of the glycosidic bond generates a second anion at N1 of the base, which generates additional unfavorable charge and increases the barrier for excision of FU. Indeed, in addition to the fluorine steric bulk, which hinders binding of FU in the hUNG active site, the unfavorable charge aspects of the transition state also contribute to its poor recognition and excision by hUNG (Drohat and Stivers, 2000; Parker *et al.*, 2007).

We suggest a multimodal toxicity mechanism for FdU leading to its unique potency. This mechanism includes (i) depletion of the thymidine nucleotide pool through inhibition of TS, preventing the repair process FU/A (and U/A) → T/A, (ii) the mispairing aspects of FU which leads to high levels of FU/G pairs, and (iii) the persistence of FU/G and FU/A pairs due to their poor reactivity with hUNG (and especially when UNG activity is inhibited). Persistence suggests that other cellular pathways act on FU lesions when these lesions are missed by hUNG during S phase. In previous studies, mismatch repair (MMR), topoisomerase 1 and TDG/SMUG1/MBD4 glycosylases have either been implicated or excluded as factors in post replication detection of FU depending on the study (Wyatt and Wilson, 2009; Huehls *et al.*, 2011; Pardee *et al.*, 2012). While prior work also suggested that TP53 mutated tumors were diagnostic for cell lines that showed the responsive hUNG phenotype, our more extensive data set paints a more complex

Molecular Pharmacology Fast Forward. Published on April 1, 2021 as DOI: 10.1124/molpharm.120.000191
This article has not been copyedited and formatted. The final version may differ from this version.

picture where TP53 loss is neither necessary or sufficient to differentiate between R and NR cells. Thus, a firm understanding of the basis for the R and NR phenotypes remains unknown and requires further experimentation.

Potential therapeutic benefits of hUNG inhibition

The observation that about 50% of our tested colorectal cancer cell lines showed increased sensitivity to FdU when hUNG was inhibited provides encouragement that hUNG might be a useful secondary target to enhance the efficacy of fluoropyrimidine therapy in colorectal cancer. Since hUNG inhibition appears to target cancers with intrinsic resistance to FdU chemotherapy, the addition of a small molecule hUNG inhibitor could improve the response rate of patients undergoing treatment in an adjuvant or metastatic setting and/or reduce dose limiting cytotoxicities.

Disclosure of Potential Conflicts of Interest

The authors report no conflicts of interest.

Authors contributions

Participated in research design: Christenson, Stivers, Eggleston, Seamon, Park

Conducted experiments: Christenson, Gizzi, Cui, Eggleston, Orris, DePasquale

Contributed new reagents or analytic tools: Christenson, Gizzi, Orris, DePasquale

Performed data analysis: Christenson, Stivers, Gizzi, Cui, Eggleston,

Wrote or contributed to the writing of the manuscript: Christenson, Stivers, Gizzi, Cui, Eggleston, Orris

Acknowledgments

The authors thank Micheal Matunis (JHSPH) for supplying purified TDG and our colleagues James Barrow (Leiber Institute), Fred Bunz (JHSOM), Vasan Yegnasubramanian (JHSOM) and James Eschleman (JHSOM) for use of key equipment, valuable discussions and reagents.

Molecular Pharmacology Fast Forward. Published on April 1, 2021 as DOI: 10.1124/molpharm.120.000191
This article has not been copyedited and formatted. The final version may differ from this version.

References

Barretina J, Caponigro G, Stransky N, Venkatesan K, Margolin AA, Kim S, Wilson CJ, Lehár J, Kryukov GV, Sonkin D, Reddy A, Liu M, Murray L, Berger MF, Monahan JE, Morais P, Meltzer J, Korejwa A, Jané-Valbuena J, Mapa FA, Thibault J, Bric-Furlong E, Raman P, Shipway A, Engels IH, Cheng J, Yu GK, Yu J, Aspesi P Jr, de Silva M, Jagtap K, Jones MD, Wang L, Hatton C, Palescandolo E, Gupta S, Mahan S, Sougnez C, Onofrio RC, Liefeld T, MacConaill L, Winckler W, Reich M, Li N, Mesirov JP, Gabriel SB, Getz G, Ardlie K, Chan V, Myer VE, Weber BL, Porter J, Warmuth M, Finan P, Harris JL, Meyerson M, Golub TR, Morrissey MP, Sellers WR, Schlegel R, and Garraway LA (2012) The Cancer Cell Line Encyclopedia enables predictive modelling of anticancer drug sensitivity. *Nature* **483**:603–607.

Benson AB 3rd, Venook AP, Cederquist L, Chan E, Chen Y-J, Cooper HS, Deming D, Engstrom PF, Enzinger PC, Fichera A, Grem JL, Grothey A, Hochster HS, Hoffe S, Hunt S, Kamel A, Kirilcuk N, Krishnamurthi S, Messersmith WA, Mulcahy MF, Murphy JD, Nurkin S, Saltz L, Sharma S, Shibata D, Skibber JM, Sofocleous CT, Stoffel EM, Stotsky-Himelfarb E, Willett CG, Wu CS, Gregory KM, and Freedman-Cass D (2017) Colon Cancer, Version 1.2017, NCCN Clinical Practice Guidelines in Oncology. *J Natl Compr Canc Netw* **15**:370–398.

Bulgar AD, Weeks LD, Miao Y, Yang S, Xu Y, Guo C, Markowitz S, Oleinick N, Gerson SL, Liu L. (2012) Removal of uracil by uracil DNA glycosylase limits pemetrexed cytotoxicity: overriding the limit with methoxyamine to inhibit base excision repair. *Cell Cell Death Dis.* **1***:e252.*

Chen WY, Wang DH, Yen RC, Luo J, Gu W, and Baylin SB (2005) Tumor suppressor HIC1 directly regulates SIRT1 to modulate p53-dependent DNA-damage responses. *Cell* **123**:437–448, Elsevier BV.

Cole AR, Ofer S, Ryzhenkova K, Baltulionis G, Hornyak P, and Savva R (2013) Architecturally diverse proteins converge on an analogous mechanism to inactivate Uracil-DNA glycosylase. *Nucleic Acids Res* **41**:8760–8775.

Datta A, Dey S, Das P, Alam SK, and Roychoudhury S (2016) Transcriptome profiling identifies genes and pathways deregulated upon floxuridine treatment in colorectal cancer cells harboring GOF mutant p53. *Genom Data* **8**:47–51.

Drohat AC, and Stivers JT (2000) Escherichia coli uracil DNA glycosylase: NMR characterization of the short hydrogen bond from His187 to uracil O2. *Biochemistry* **39**:11865–11875.

Fischer F, Baerenfaller K, and Jiricny J (2007) 5-Fluorouracil is efficiently removed from DNA by the base excision and mismatch repair systems. *Gastroenterology* **133**:1858–1868.

Geng L, Huehls AM, Wagner JM, Huntoon CJ, and Karnitz LM (2011) Checkpoint signaling, base excision repair, and PARP promote survival of colon cancer cells treated with 5-fluorodeoxyuridine but not 5-fluorouracil. *PLoS One* **6**:e28862.

Molecular Pharmacology Fast Forward. Published on April 1, 2021 as DOI: 10.1124/molpharm.120.000191
This article has not been copyedited and formatted. The final version may differ from this version.

Grogan BC, Parker JB, Guminski AF, and Stivers JT (2011) Effect of the thymidylate synthase inhibitors on dUTP and TTP pool levels and the activities of DNA repair glycosylases on uracil and 5-fluorouracil in DNA. *Biochemistry* **50**:618–627.

Houghton JA, Houghton PJ, and Wooten RS (1979) Mechanism of induction of gastrointestinal toxicity in the mouse by 5-fluorouracil, 5-fluorouridine, and 5-fluoro-2′-deoxyuridine. *Cancer Res* **39**:2406–2413.

Huehls AM, Huntoon CJ, Joshi PM, Baehr CA, Wagner JM, Wang X, Lee MY, and Karnitz LM (2016) Genomically Incorporated 5-Fluorouracil that Escapes UNG-Initiated Base Excision Repair Blocks DNA Replication and Activates Homologous Recombination. *Mol Pharmacol* **89**:53–62.

Huehls AM, Wagner JM, Huntoon CJ, Geng L, Erlichman C, Patel AG, Kaufmann SH, and Karnitz LM (2011) Poly(ADP-Ribose) Polymerase Inhibition Synergizes with 5-Fluorodeoxyuridine but not 5-Fluorouracil in Ovarian Cancer Cells. *Cancer Res* **71**:4944-54.

Kaldate RR, Haregewoin A, Grier CE, Hamilton SA, and McLeod HL (2012) Modeling the 5-Fluorouracil Area Under the Curve Versus Dose Relationship to Develop a Pharmacokinetic Dosing Algorithm for Colorectal Cancer Patients Receiving FOLFOX6. *Oncologist* **17**:296-302.

Kavli B, Sundheim O, Akbari M, Otterlei M, Nilsen H, Skorpen F, Aas PA, Hagen L, Krokan HE, and Slupphaug G (2002) hUNG2 Is the Major Repair Enzyme for Removal of Uracil from U:A Matches, U:G Mismatches, and U in Single-stranded DNA, with hSMUG1 as a Broad Specificity Backup. *J Biol Chem* **277**:39926-36.

Kim H-Y, Cho Y, Kang H, Yim Y-S, Kim S-J, Song J, and Chun K-H (2016) Targeting the WEE1 kinase as a molecular targeted therapy for gastric cancer. *Oncotarget* **7**:49902–49916.

Longley DB, Harkin DP, and Johnston PG (2003) 5-fluorouracil: mechanisms of action and clinical strategies. *Nat Rev Cancer* **3**:330–338.

Maley F (1962) Nucleotide interconversions VII. The effect of halogenated and N-methyl derivatives of deoxycytidylic acid on deoxycytidylate deaminase and thymidylate synthetase. *Biochim Biophys Acta* **61**:135-8.

Meyers M, Wagner MW, Mazurek A, Schmutte C, Fishel R, and Boothman DA (2005) DNA mismatch repair-dependent response to fluoropyrimidine-generated damage. *J Biol Chem* **280**:5516–5526.

Mojardín L, Botet J, Quintales L, Moreno S, and Salas M (2013) New insights into the RNA-based mechanism of action of the anticancer drug 5'-fluorouracil in eukaryotic cells. *PLoS One* **8**:e78172.

Mol CD, Arvai AS, Sanderson RJ, Slupphaug G, Kavli B, Krokan HE, Mosbaugh DW, and Tainer JA (1995) Crystal structure of human uracil-DNA glycosylase in complex with a protein inhibitor: protein mimicry of DNA. *Cell* **82**:701–708.

Molecular Pharmacology Fast Forward. Published on April 1, 2021 as DOI: 10.1124/molpharm.120.000191
This article has not been copyedited and formatted. The final version may differ from this version.

Morgan MT, Bennett MT, and Drohat AC (2007) Excision of 5-halogenated uracils by human thymine DNA glycosylase. Robust activity for DNA contexts other than CpG. *J Biol Chem* **282**:27578–27586.

Myers CE, Young RC, and Chabner BA (1975) Biochemical determinants of 5-fluorouracil response in vivo. The role of deoxyuridylate pool expansion. *J Clin Invest* **56**:1231–1238.

Neri F, Incarnato D, Krepelova A, Rapelli S, Anselmi F, Parlato C, Medana C, Dal Bello F, and Oliviero S (2015) Single-base resolution analysis of 5-formyl and 5-carboxyl cytosine reveals promoter DNA methylation dynamics. *Cell Rep* **10**:674–683.

Pardee TS, Gomes E, Jennings-Gee J, Caudell D, and Gmeiner WH (2012) Unique dual targeting of thymidylate synthase and topoisomerase1 by FdUMP[10] results in high efficacy against AML and low toxicity. *Blood* **119**:3561–3570.

Parker JB, Bianchet MA, Krosky DJ, Friedman JI, Amzel LM, and Stivers JT (2007) Enzymatic capture of an extrahelical thymine in the search for uracil in DNA. *Nature* **449**:433–437.

Parker JB, and Stivers JT (2011) Dynamics of uracil and 5-fluorouracil in DNA. *Biochemistry* **50**:612–617.

Pritchard DM, Watson AJ, Potten CS, Jackman AL, and Hickman JA (1997) Inhibition by uridine but not thymidine of p53-dependent intestinal apoptosis initiated by 5-fluorouracil: evidence for the involvement of RNA perturbation. *Proc Natl Acad Sci U S A* **94**:1795–1799.

Slupphaug G, Eftedal I, Kavli B, Bharati S, Helle NM, Haug T, Levine DW, and Krokan HE (1995) Properties of a recombinant human uracil-DNA glycosylase from the UNG gene and evidence that UNG encodes the major uracil-DNA glycosylase. *Biochemistry* **34**:128–138.

Sommer H, and Santi DV (1974) Purification and amino acid analysis of an active site peptide from thymidylate synthetase containing covalently bound 5-fluoro-2′-deoxyuridylate and methylenetetrahydrofolate. *Biochem Biophys Res Commun* **57**:689-95.

Sowers LC, Eritja R, Kaplan B, Goodman MF, and Fazakerly GV (1988) Equilibrium between a wobble and ionized base pair formed between fluorouracil and guanine in DNA as studied by proton and fluorine NMR. *J Biol Chem* **263**:14794–14801.

Subramanian A, Tamayo P, Mootha VK, Mukherjee S, Ebert BL, Gillette MA, Paulovich A, Pomeroy SL, Golub TR, Lander ES, and Mesirov JP (2005) Gene set enrichment analysis: a knowledge-based approach for interpreting genome-wide expression profiles. *Proc Natl Acad Sci U S A* **102**:15545–15550.

Van Cutsem E, Cunningham D, Maroun J, Cervantes A, and Glimelius B (2002) Raltitrexed: current clinical status and future directions. *Ann Oncol* **13**:513–522.

van Groeningen CJ, Peters GJ, Leyva A, Laurensse E, and Pinedo HM (1989) Reversal of 5-fluorouracil-induced myelosuppression by prolonged administration of high-dose uridine. *JNCI: Journal of the National Cancer Institute* **81**:157–162.

van Laar JAM, Rustum YM, Ackland SP, van Groeningen CJ, and Peters GJ (1998) Comparison of 5-fluoro-2′-deoxyuridine with 5-fluorouracil and their role in the treatment of colorectal cancer. *Eur J Cancer* **34**:296–306.

Vodenkova S, Buchler T, Cervena K, Veskrnova V, Vodicka P, and Vymetalkova V (2020) 5-fluorouracil and other fluoropyrimidines in colorectal cancer: Past, present and future. *Pharmacol Ther* **206**:107447.

Weeks LD, Zentner GE, Scacheri PC, and Gerson SL (2014) Uracil DNA glycosylase (UNG) loss enhances DNA double strand break formation in human cancer cells exposed to pemetrexed. *Cell Death Dis* **5**:e1045.

Weil AF, Ghosh D, Zhou Y, Seiple L, McMahon MA, Spivak AM, Siliciano RF, and Stivers JT (2013) Uracil DNA glycosylase initiates degradation of HIV-1 cDNA containing misincorporated dUTP and prevents viral integration. *Proc Natl Acad Sci U S A* **110**:E448-E457

Weiser BP, Rodriguez G, Cole PA, and Stivers JT (2018) N-terminal domain of human uracil DNA glycosylase (hUNG2) promotes targeting to uracil sites adjacent to ssDNA--dsDNA junctions. *Nucleic Acids Res* **46**:7169–7178.

Wyatt MD, and Wilson DM III (2009) Participation of DNA repair in the response to 5-fluorouracil. *Cell Mol Life Sci* **66**:788–799, Springer Science and Business Media LLC.

Yan Y, Han X, Qing Y, Condie AG, Gorityala S, Yang S, Xu Y, Zhang Y, and Gerson SL (2016) Inhibition of uracil DNA glycosylase sensitizes cancer cells to 5-fluorodeoxyuridine through replication fork collapse-induced DNA damage. *Oncotarget* **7**:59299–59313.

Yan, Yan Y, Qing Y, Pink JJ, and Gerson SL (2018) Loss of Uracil DNA Glycosylase Selectively Resensitizes p53-Mutant and -Deficient Cells to 5-FdU. *Mol Cancer Res* **16***:212-221.*

Molecular Pharmacology Fast Forward. Published on April 1, 2021 as DOI: 10.1124/molpharm.120.000191
This article has not been copyedited and formatted. The final version may differ from this version.

Footnotes

This work was supported by NIH grant RO1-GM056834 (J.T.S.). EC is supported in part by a McMillan Cancer Fellowship from Johns Hopkins. A.G is supported by an NRSA Ruth Kirschstein Fellowship F32AI150561. B.O. is supported by NIH Training Grant T32 GM007445.

The authors, Anthony Gizzi, Junru Cui and Matthew Egleston contributed equally to the work.

The authors have no conflict of interest.

Molecular Pharmacology Fast Forward. Published on April 1, 2021 as DOI: 10.1124/molpharm.120.000191
This article has not been copyedited and formatted. The final version may differ from this version.

Figure Legends

Figure 1. Metabolism of FU and FdU and inhibitors of hUNG. (A) Metabolic reactions of FU and FdU leading to the RNA and DNA pathways for cellular toxicity. **(B)** hUNG can be inhibited in human cells by expression of the small PBS2 bacteriophage protein UGI (blue) which targets the active site of hUNG (PDB 1UGH). **(c)** Small molecule inhibitors of hUNG have been characterized that also target the same site as UGI (PDB 3FCI). Abbreviations: FU; 5-fluorouracil, FdU; 5-fluorodeoxyuridine, FUMP; 5-fluorouridine monophosphate, FUDP; 5-fluorouridine diphosphate, FUTP; 5-fluorouridine triphosphate, FdUMP; 5-fluorodeoxyuridine monophosphate, FdUDP; 5-fluorodeoxyuridine diphosphate, FdUTP; 5-fluorodeoxyuridine triphosphate, NMPK; Nucleoside monophosphate kinase, NDPK; nucleoside diphosphate kinase, OPRT; orotate phosphoribosyltransferase, polε: DNA polymerase epsilon, polδ; polymerase delta, TK; thymidine kinase, TS; thymidylate synthase, RNR; ribonucleotide reductase, RNAP III; RNA polymerase III, RTX; raltitrexed, dUMP; deoxyuridine monophosphate, dTMP; deoxythymidine monophosphate, dUDP; deoxyuridine diphosphate, dUTP; deoxyuridine triphosphate.

Figure 2. Inhibition of hUNG activity by UGI inducible expression increases potency of FdU but not FU for a subset of colorectal cancer cell lines. (A) UNG activity assay performed on protein lysates from parental (WT) colon cancer cell lines or the constructs containing doxycycline inducible UGI. This assay uses a 5'-FAM labeled 19mer ssDNA substrate containing a central uracil base. When hUNG activity is present a 5'-FAM labeled 9mer product is produced after sample processing which is resolved from substrate by denaturing polyacrylamide gel electrophoresis. Abbreviations: NI, not induced; I, doxycycline induced. **(B)** Dose-response curves for responsive colon cancer cell lines exposed to FdU under hUNG active **(**black**)** and inhibited (red) conditions. **(C)** Dose-response curves for non-responsive colon cancer cell lines exposed to FdU under hUNG active **(**black**)** and inhibited (red) conditions. **(D)** Dose-response curves for FdU responsive colon cancer cell lines exposed to FU under hUNG active **(**black**)** and inhibited (red) conditions. Each dose-response curve was repeated at least three times beginning from a fresh culture of each cell line. The error bars on each data point are the standard deviation of three technical replicates from the same biological replicate. Overall, three biological replicates were performed (**Supplemental Table S2**)

Molecular Pharmacology Fast Forward. Published on April 1, 2021 as DOI: 10.1124/molpharm.120.000191
This article has not been copyedited and formatted. The final version may differ from this version.

Figure 3. LC/MS measurements of U and FU bases in DNA of responsive (R) and non-responsive (NR) lines in the presence or absence of hUNG inhibition or FdU treatment. **(A)** Genomic U content of responsive DLD1 and HT29 lines and non-responsive LoVo and SW620 lines in the presence and absence of FdU treatment and hUNG inhibition as indicated. **(B)** Genomic FU content of responsive DLD1 and HT29 lines and non-responsive LoVo and SW620 lines in the presence and absence of FdU treatment and hUNG inhibition as indicated. In these experiments, cells were synchronized at the G1/S border by serum starvation for 48 h, followed by return to normal media for 2h and supplementation with 5 μM FdU for 24 h before harvesting genomic DNA. The error bars on each measurement represent the standard deviation from two biological replicates from two distinct experiments started from a fresh culture of each cell line/condition.

Figure 4. Cell killing by raltitrexed (RTX) for a subset of FdU responsive colorectal cancer cell lines in the presence and absence of hUNG activity. **(A)** Dose-response curves for RTX for the responsive colon cancer lines that demonstrated increased sensitivity to FdU upon hUNG inhibition. **(B)** Dose-response curves for the non-responsive colon cancer cell lines that demonstrated no change in sensitivity to FdU upon hUNG inhibition. Each dose-response curve was repeated at least twice beginning from a fresh culture of each cell line. The error bars on each measurement represent the standard deviation from three technical replicates of each cell line/condition.

Figure 5. Comparison of FdU, FU or RTX responses of hUNG R and NR colon cancer lines. (**A**) FdU IC50 values for R and NR lines in absence (black) and presence (red) of hUNG inhibition. (**B**) FU IC50 values for R and NR lines in absence and presence of hUNG inhibition. (**C**) RTX AUC values for R and NR in absence and presence of hUNG inhibition. Error bars are the SD of three (FdU) and two (FU, RTX) biological replicates from distinct experiments started from a fresh cell culture. A student's T-test was performed to compare the difference between the FdU IC50 in the six responsive and six non-responsive lines when hUNG was active (p-value = 0.002). The change in raltitrexed AUC with hUNG inhibition between the FdU responsive and nonresponsive cell lines was compared using a student's T-test (p-value = 0.03).

Molecular Pharmacology Fast Forward. Published on April 1, 2021 as DOI: 10.1124/molpharm.120.000191
This article has not been copyedited and formatted. The final version may differ from this version.

Figure 6. Differential effects of dT and dU supplementation on toxicities of FdU, FU, and RTX in the hUNG responsive DLD1 and HT29 cell lines. (a) LC/MS measurements of U and FU bases in DNA in DLD1 and HT29 cells treated with FdU in the absence and presence of hUNG activity. These measurements were performed with and without supplementation with 100 μM dU or dT as indicated in the legend. Two biological replicate measurements were made. **(b)** Supplementation with 100 μM dT increases the IC_{50} of FdU and removes the response to hUNG inhibition (red curves). In contrast, dT supplementation completely rescues the toxicity of RTX while having no impact on FU toxicity. Dose response curves for these cell lines under hUNG active and inhibited conditions are shown by the dashed lines for comparison. **(c)** Supplementation with 100 μM dU increases the IC_{50} of FdU, but the response to hUNG inhibition (red curves) is retained. In contrast, dU supplementation with FU does not alter toxicity in the DLD1 cell line but slightly enhances toxicity in the HT29 line. Supplementation with 100 μM dU during treatment with RTX increases the IC_{50} by 100-fold but retains the increased AUC under conditions of hUNG inhibition (red curves) observed with RTX alone (see text). The supplementation experiments with FdU were performed in biological triplicates (three technical replicates for each) and supplementation experiments with FU and RTX were performed with biological duplicates (three technical replicates for each).

Figure 7. hUNG activity on U, FU and BrU DNA bases and cell toxicities of dU and BrdU. (A) 19mer substrates containing U, FU, or BrU were reacted with 50 pM of hUNG catalytic domain for the indicated times and the reaction products were resolved by gel electrophoresis after processing. The excision of the base results in a 5'-FAM labeled 9mer product. **(B)** $HT29^{UGI}$ and $DLD1^{UGI}$ cells were dosed with dU and BrdU in the presence **(**black**)** and absence (red) of hUNG activity. After 72 hours of nucleoside exposure cell viability was measured using the MTS assay. Each concentration-response curve was repeated at least twice beginning from a fresh culture of each cell line. The error bars on each measurement represent the standard deviation from three technical replicates of each cell line/condition.

Figure 8. Sensitivity of cells to FdU upon loss of thymidine DNA glycosylase (TDG). (A) Western blot demonstrating loss of TDG protein expression with two independent clones generated with unique CRISPR guides targeting the TDG coding sequence ($DLD1^{UGI}$ cell line) A negative control guide sequence is also shown. (**B**) Western blot establishing reduced TDG expression following introduction of two unique TDG shRNA coding sequences into $HT29^{UGI}$ and $DLD1^{UGI}$ cells. Expression in the control guide shRNA and the parental cell lines (wt) are also

Molecular Pharmacology Fast Forward. Published on April 1, 2021 as DOI: 10.1124/molpharm.120.000191
This article has not been copyedited and formatted. The final version may differ from this version.

shown. (**C)** DLD^{UGI} cells containing two unique CRISPR TDG knock-outs were exposed to a spectrum of FdU concentrations in a hUNG active (black data) and inhibited (red data) background. Cells were exposed to drug for 72 hours before determination of viability using the MTS assay and shRNA negative controls are also shown. (**D**) $HT29^{UGI}$ and $DLD1^{UGI}$ cells expressing shRNA targeting TDG were exposed to a spectrum of FdU concentrations in a hUNG active (black data) and inhibited (red data) background. Cells were exposed to drug for 72 hours before determination of viability using the MTS assay and shRNA negative controls are also shown. Each dose-response curve was repeated at least twice beginning from a fresh culture of each cell line. The error bars on each measurement represent the standard deviation from three technical replicates of each cell line/condition.

Molecular Pharmacology Fast Forward. Published on April 1, 2021 as DOI: 10.1124/molpharm.120.000191
This article has not been copyedited and formatted. The final version may differ from this version.

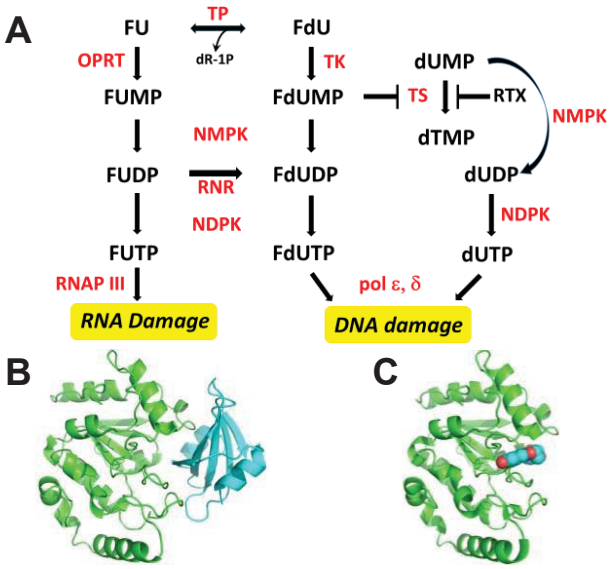

Fig 1

Molecular Pharmacology Fast Forward. Published on April 1, 2021 as DOI: 10.1124/molpharm.120.000191
This article has not been copyedited and formatted. The final version may differ from this version.

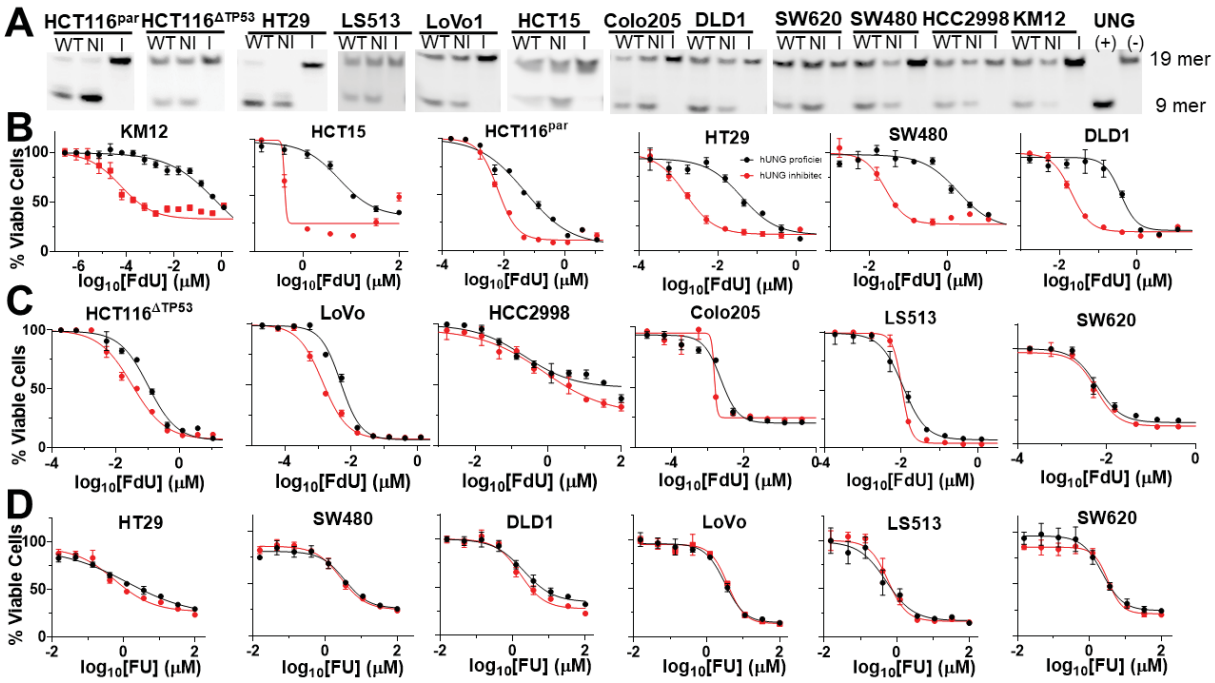

Fig. 2

Molecular Pharmacology Fast Forward. Published on April 1, 2021 as DOI: 10.1124/molpharm.120.000191
This article has not been copyedited and formatted. The final version may differ from this version.

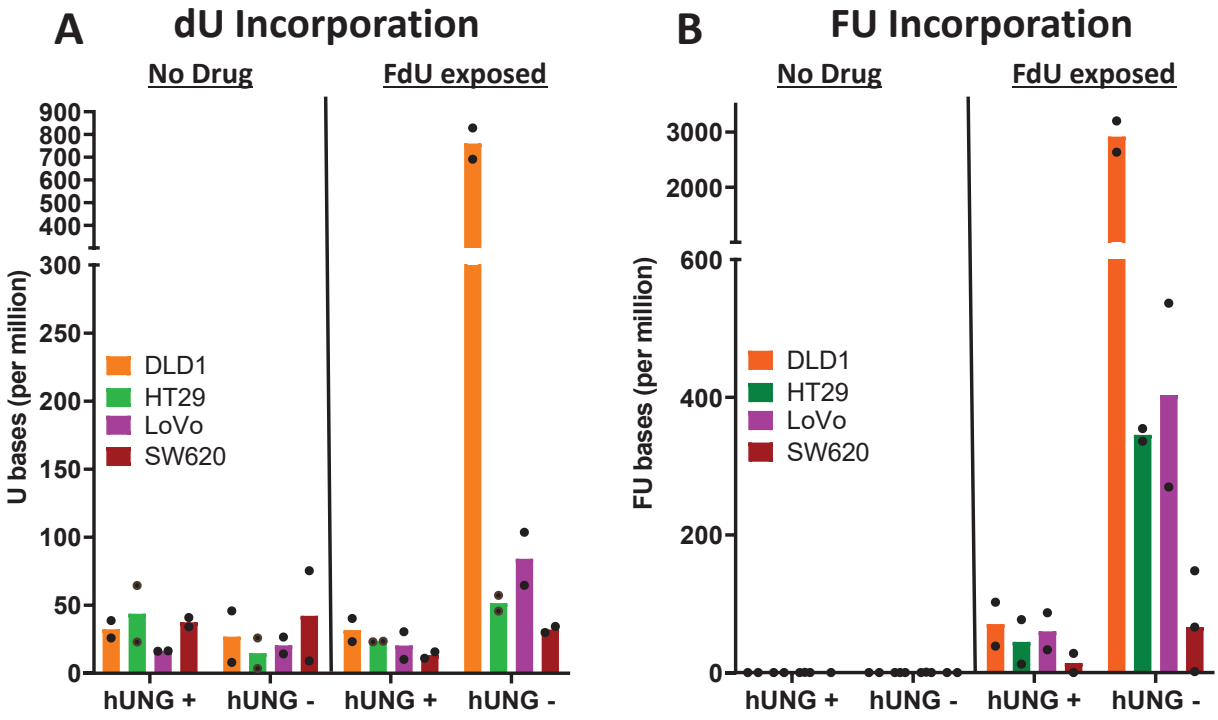

Fig. 3

Molecular Pharmacology Fast Forward. Published on April 1, 2021 as DOI: 10.1124/molpharm.120.000191
This article has not been copyedited and formatted. The final version may differ from this version.

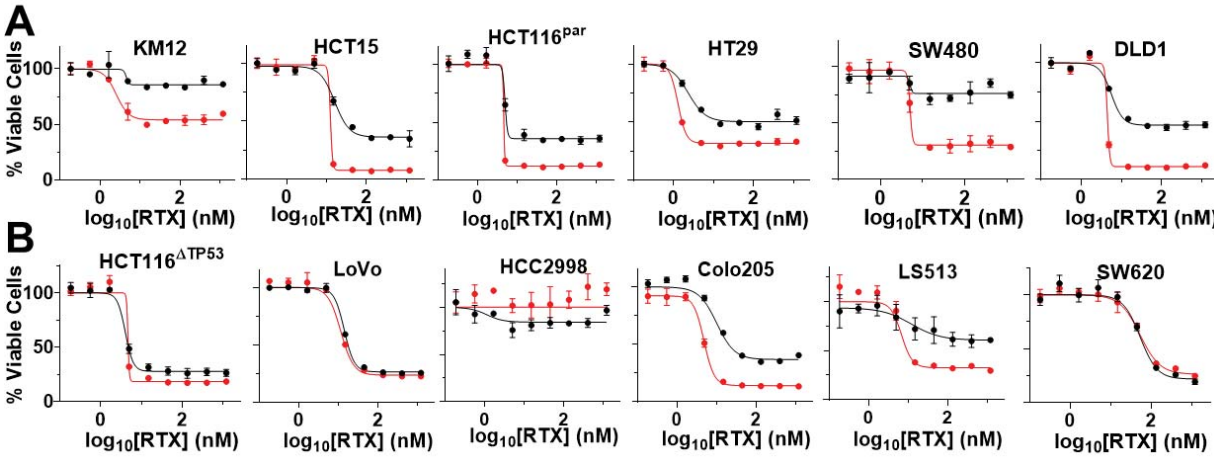

Fig. 4

Molecular Pharmacology Fast Forward. Published on April 1, 2021 as DOI: 10.1124/molpharm.120.000191
This article has not been copyedited and formatted. The final version may differ from this version.

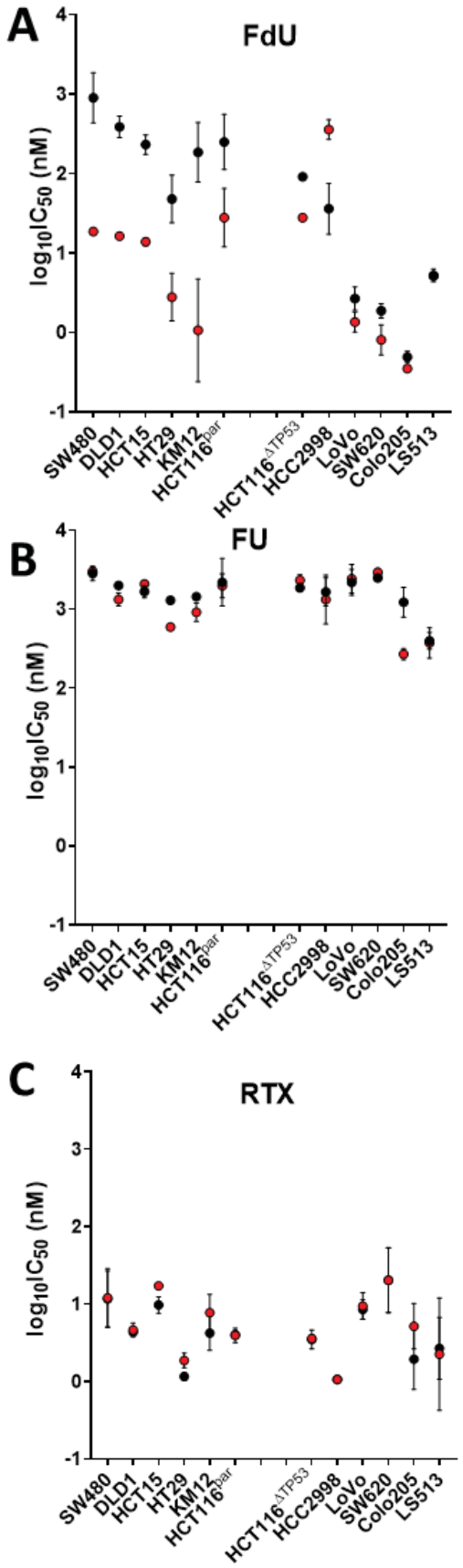

Molecular Pharmacology Fast Forward. Published on April 1, 2021 as DOI: 10.1124/molpharm.120.000191
This article has not been copyedited and formatted. The final version may differ from this version.

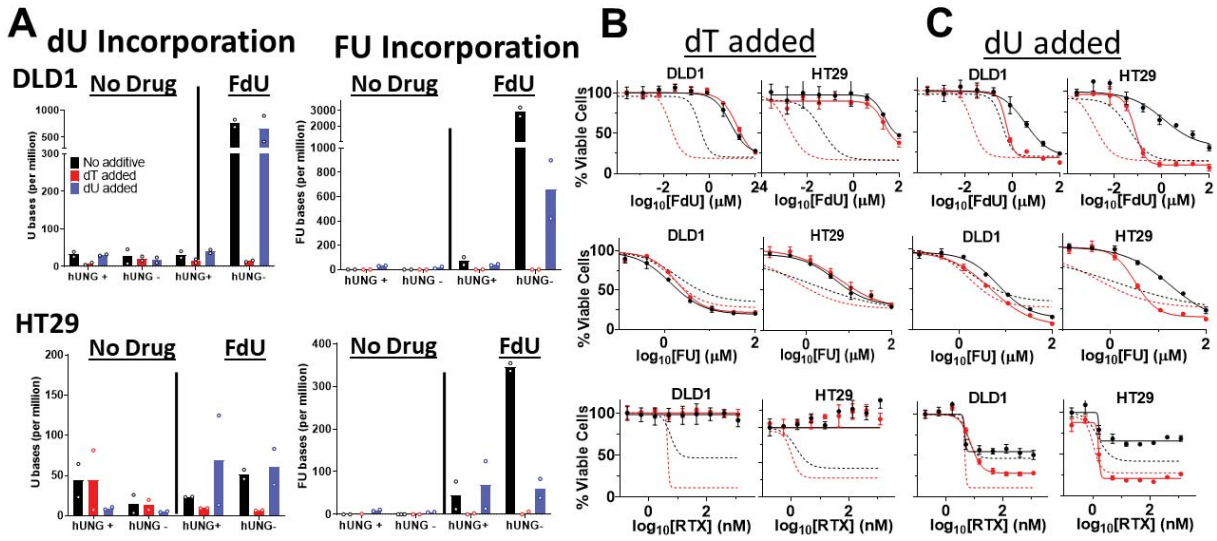

Fig. 6

Molecular Pharmacology Fast Forward. Published on April 1, 2021 as DOI: 10.1124/molpharm.120.000191
This article has not been copyedited and formatted. The final version may differ from this version.

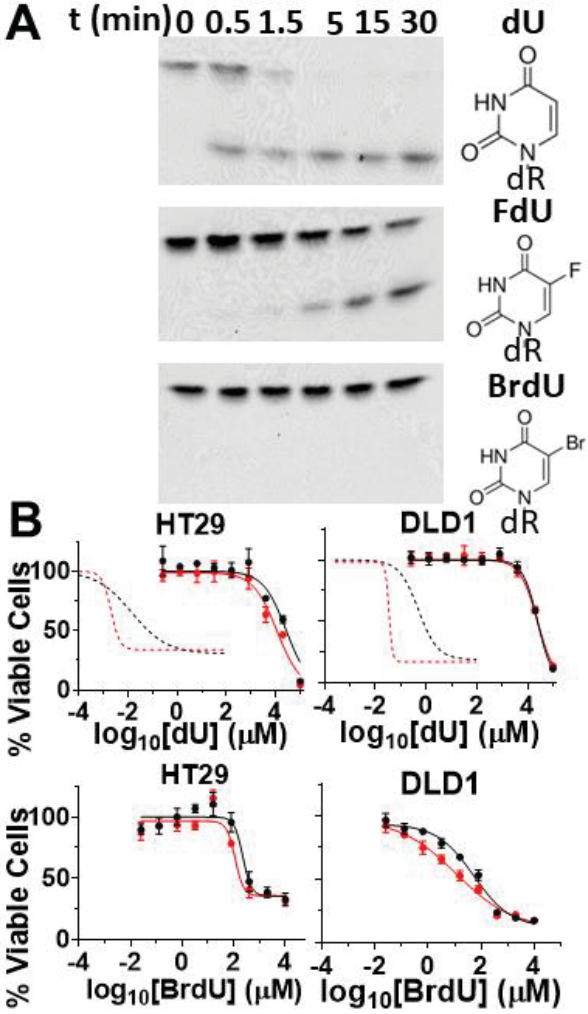

Fig. 7

Molecular Pharmacology Fast Forward. Published on April 1, 2021 as DOI: 10.1124/molpharm.120.000191
This article has not been copyedited and formatted. The final version may differ from this version.

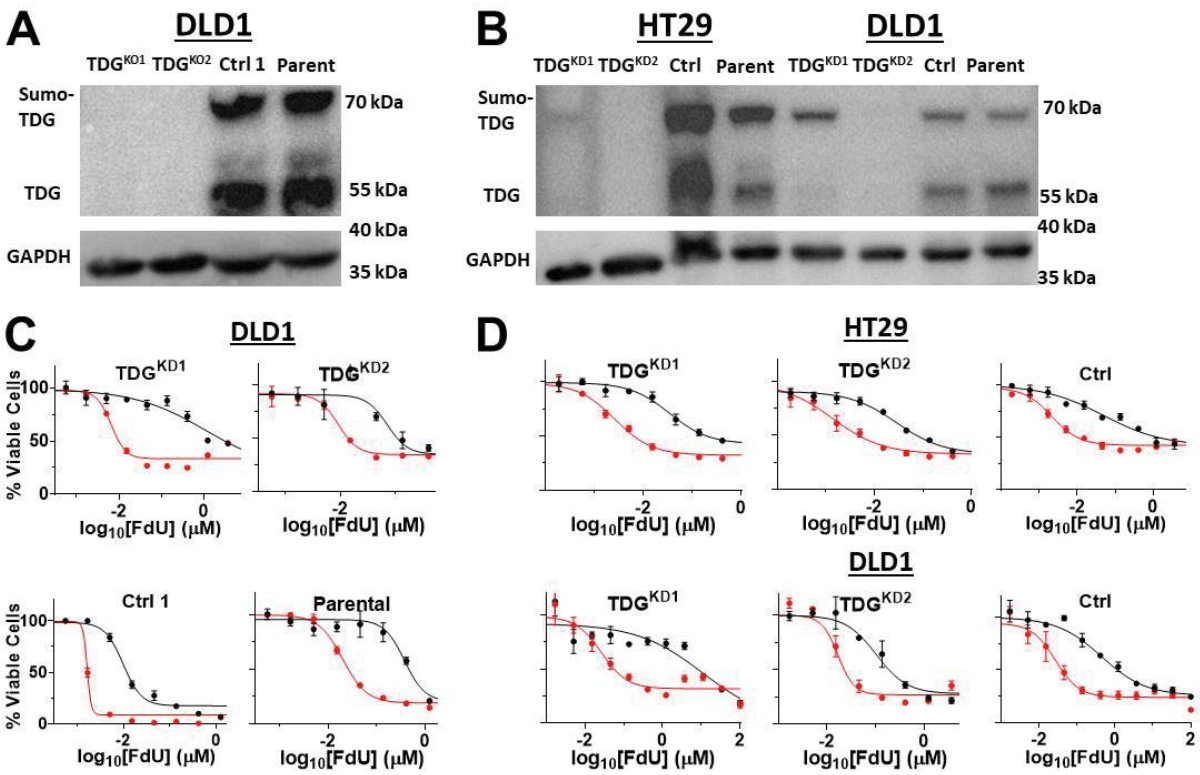

Fig. 8